CERN-ACC-2016-0041

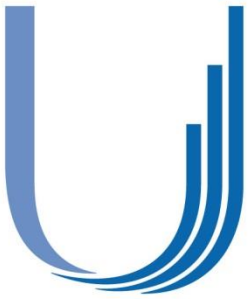

LHC Injectors Upgrade

Technical Design Report

Vol. II: Ions

CERN-ACC-2016-0041
01/04/2016

Editors

J. Coupard, H. Damerau, A. Funken, R. Garoby,
S. Gilardoni, B. Goddard, K. Hanke, D. Manglunki,
M. Meddahi, G. Rumolo, R. Scrivens, E. Shaposhnikova

April 2016
EDMS 1626950

LHC Injectors Upgrade

Technical Design Report

S. Albright, M. E. Angoletta, G. Arduini, T. Argyropoulos, J. Axensalva, W. Bartmann, H. Bartosik, P. Baudrenghien, G. Bellodi, A. Blas, D. Bodart, M. Bodendorfer, T. Bohl, J. Borburgh, A. Butterworth, C. Carli, E. Carlier, K. Cornelis, J. Coupard, J. M. Cravero, H. Damerau, S. Deleval, J. Devine, C. Di Paolo, L. Ducimetiere, A. Dworak, A. Findlay, R. Froeschl, A. Funken, R. Garoby, F. Gerigk, S. Gilardoni, B. Goddard, A. Guerrero Ollacarizqueta, G. Hagmann, S. Hancock, K. Hanke, J. Hansen, M. Hasse, W. Hoefle, E. B. Holzer, A. Huschauer, M. Jaussi, E. Jensen, S. Jensen, R. Jones, J. Jowett, V. Kain, I. Kobzeva, G. Kotzian, D. Küchler, J.-M. Lacroix, M. Lamont, K. Li, A. Lombardi, M. Maintrot, D. Manglunki, S. Maridor, S. Mataguez, M. Meddahi, R. Mompo, M. Morvillo, F. X. Nuiry, M. Paoluzzi, S. Pasinelli, D. Perrelet, A. Perillo Marcone, S. Pittet, T. Rijoff, F. Roncarolo, C. Rossi, G. Rumolo, S. Sadovich, R. Scrivens, E. Shaposhnikova, R. Steerenberg, G. Sterbini, V. Toivanen, G. Tranquille, J. Uythoven, F. M. Velotti, J. Vollaire.

Contents

1 Executive Summary

The HL-LHC request of integrated luminosity with Pb-Pb collisions in the post-LS2 era can be met with the parameters summarized in Table 1.1 [1] of the Pb beam at the SPS extraction.

Table 1.1 Pb ion beam parameters at SPS extraction for the HL-LHC project.

Beam structure	50 ns bunch trains at LHC injection
Number of bunches (n_b)	1248
Ions/bunch (N)	$2.1 \cdot 10^8$
Transverse emittance ($\varepsilon_{x,y}$) [μm]	1.3

The following set of LIU baseline upgrades are aimed at matching the achievable Pb ion beam parameters at the SPS extraction with those requested by HL-LHC, as well as improving the availability of the ion injector chain:

1. **Source and Linac3**: Improvement of the Low Energy Beam Transport (LEBT); Increase of the injection rate from Linac3 into the Low Energy Ion Ring (LEIR) from 5 to 10 Hz; Renovation of the spectrometer line ('LBS') for energy measurements;
2. **LEIR**: Transmission improvement; Beam loss reduction; Installation of an external dump; Instrumentation improvements;
3. **PS**: Bunch splitting;
4. **SPS**: Momentum slip stacking; Reduction of injection kicker rise time from 225 to 150 ns; Mitigation of losses.

In addition, the following two options (not part of the LIU baseline) have been considered, since they were identified to potentially further boost the operational performance:

1. **Use batch compression to 50 ns** at top energy in the PS, which leads to 25 ns spacing in LHC after slip stacking in the SPS and requires the installation of a new broad-band cavity in the PS;
2. **Reduce the minimum spacing** between injected batches in the SPS to 100 ns, which requires the installation of a new injection system in the SPS.

Both these options are detailed in Chapter 7 of this TDR. Option 1 is being further explored regarding feasibility and it has also been analysed in terms of reachable beam parameters. Option 2 is not being pursued, as it can only provide a marginal gain relative to its cost, after the deployment of the 150 ns rise time improvement of the SPS injection system in 2015.

Table 1.2 summarises a set of achievable beam parameters at the LHC injection as well as some machine parameters and the estimated luminosity reach for different relevant scenarios [1],[2],[3]. The LHC performance efficiency (η), defined as the percentage of scheduled physics time spent on successful fills (including the minimum turn-around time) [4], has been also included in the table. The complete list of beam parameters through the LHC ion injector chain (i.e. at injection and extraction from each machine) has been included in Section 7.3 of this document. The column labelled 'No upgrade' provides the average beam parameter values achieved in 2015 over the last few days of the Pb ion run, when the injectors performance had been carefully tuned and optimised. The LIU reach with the baseline upgrades listed above is displayed in the 'LIU-ions' column, while 'LIU-ions 25 ns' shows the achievable values if Option 1 is included in the upgrade program. Finally, the 'HL-LHC' column summarises the requested HL-LHC parameters, already introduced above, and the associated integrated luminosity. For completeness, the estimated maximum number of bunches in LHC and the minimum LHC filling time

for each of these scenarios have been also reported in the table. To be noted that the value of LHC performance efficiency has been chosen to be 62% in the first three columns, because this is the value achieved in 2015, while it was assumed to be 50% in the HL-LHC column (same as for proton operation) [3].

Table 1.2 Estimated performance reach for the different scenarios.

Parameters	**No upgrade**	**LIU-ions**	**LIU-ions 25 ns**	**HL-LHC**
Injection filling pattern – ns	12t x (2b x 100 + 150)	6t x (8b x 50 + 100)	7t x (8b x 25 + 125)	48b x 50
Number of bunches	518	1152	1680	1248
LHC performance efficiency – η	62%	62%	62%	50%
Bunch intensity (RMS) – ions/bunch	2.2×10^8	1.7×10^8	1.7×10^8	2.1×10^8
Normalised emittance (x and y) (mean) – μm	1.45	1.3	1.3	1.3
LHC filling time – min	40	45	60	45
Estimated maximum achievable integrated luminosity/year – nb^{-1}	~1.3	~2.4	~3.5	~2.9

Compared to the HL-LHC request, the baseline LIU-ions scenario gives 20% lower bunch intensities at the SPS extraction and 8% fewer bunches in LHC, leading to ~15% lower integrated luminosity [3].
The LIU-ions 25 ns scenario Option 1 compensates the 20% lower bunch intensities with up to 35% more bunches in LHC, resulting in a ~20% higher integrated luminosity than the requested value (estimation based on a simple scaling with the total number of bunches). This preliminary estimate suggests that this option has the potential to meet the final requirement of integrated luminosity during the post-LS2 era and even allows for some margin against the main risks of the project (mitigation of losses throughout the injector chain, SPS slip stacking, and preservation of high LHC performance efficiency).

The installation of the LIU-ions equipment will take place during the (Extended) Year-End Technical Stops ((E)YETS) 2016-17 and 2017-18, and during the Long Shutdown 2 (LS2) in 2019 and 2020. The Cost to Completion of the LIU-ions chain baseline upgrade amounts to 3 MCHF.

1.1 References

[1] J.M. Jowett, *HL-LHC heavy-ion beam parameters at LHC injection*, EDMS 1525065 (2015).

[2] H. Bartosik, B. Goddard and G. Rumolo, *LIU beam ion specifications*, in LIU Beam Parameter Working Group meeting, 12 February 2016, CERN (2016).

[3] H. Bartosik et al, *LIU beam parameters specifications for ions at the exit of the SPS*, EDMS 1581381 (2016).

[4] G. Arduini et al, *Beam parameters at LHC Injection*, CERN-ACC-2014-0006 (2014).

2 LIU-ions Technical Design Report – Introduction

2.1 LIU-ions upgrade: Goal and means

A detailed analysis to provide estimates for the HL-LHC request of integrated luminosity with Pb-Pb collisions, and for the required Pb beam parameters at the SPS extraction to fulfil this target, has been carried out in [1]. In particular, the HL-LHC target has been based on a future running scenario assumed after the ALICE upgrade in LS2 [2], which aims at accumulating an integrated luminosity of 10 nb^{-1} over the Pb-Pb ion runs between LS2 and LS4, together with the other requirements summarised in Table 2.1.

Table 2.1 Condensed summary of the experiments' requirements.

Description	**ALICE**	**CMS**	**ATLAS**
Maximum hadronic interaction rate	50 kHz in Pb-Pb	50 kHz in Pb-Pb	-
Peak luminosity	$7.x10^{27}$ $cm^{-2}s^{-1}$	$7.x10^{27}$ $cm^{-2}s^{-1}$	-
Integrated luminosity (Pb-Pb) from LS2 to LS4	10 nb^{-1}	10 nb^{-1}	10 nb^{-1}
Other requests	one Pb-Pb run at reduced magnetic field one p-Pb run with about 50 nb-1 One pp reference run at (82/208)x(top energy)	p-Pb	p-Pb
Duration of run / year	"one month" LHC heavy ion operation (=24 days)	24 days	24 days

Since only four Pb-Pb runs will take place between LS2 and LS4, and one of them will be conducted with reduced magnetic field, the resulting request for yearly integrated luminosity was estimated to be about 2.85 nb^{-1}/year. In brief, the simplified model described in [1] translates this requirement into the desired Pb ion beam parameters at the SPS extraction specified in Table 2.2.

Table 2.2 Pb ion beam parameters at SPS extraction for the HL-LHC project.

Beam structure	50 ns bunch trains at LHC injection
Number of bunches (n_b)	1248
Ions/bunch (N)	$2.1 \cdot 10^8$
Transverse emittance ($\varepsilon_{x,y}$) [μm]	1.3

In present operation and after few significant improvements implemented during the 2015 run, the Pb ion beam parameters achieved at the SPS extraction [3] are summarized in Table 2.3.

Table 2.3 Achieved Pb ion beam parameters at SPS extraction (2015).

Beam structure	100/150 ns bunch trains at LHC injection
Number of bunches (n_b)	518
Ions/bunch (N)	$2.2 \cdot 10^8$
Transverse emittance ($\varepsilon_{x,y}$) [μm]	1.45

Comparing Table 2.2 and Table 2.3, we conclude that the HL-LHC target is roughly the same intensity per bunch within a 10% lower transverse emittance, but notably a 2.4 times larger number of bunches in the LHC.

In an effort to match the Pb ion beam parameters at the SPS extraction with those requested by HL-LHC, the following upgrades have been planned within the LIU project (detailed in the next chapters):

- Improvement of the Low Energy Beam Transport (LEBT);
- Increase the injection rate from Linac3 into LEIR from 5 to 10 Hz (the so called "*100 ms operation*");
- Improvement of the LEIR transmission by understanding and mitigating the present intensity limitation;
- Bunch splitting in the PS;
- Momentum slip stacking in the SPS;
- Mitigation of losses in the SPS.

In addition, the following items have been also endorsed within the injector upgrade program, which are expected to benefit operational performance and availability of the ion injector chain in the post-LS2 era:

- The construction of an oven test stand, in order to test various changeover strategies;
- The renovation of the LBS spectrometer line for energy measurements, as the current one will no longer be used when Linac2 will stop operating after LS2;
- The design, construction and installation of a clean beam dump for the beam extracted from LEIR.

The evolution of the Pb ion beam characteristics throughout the injector chain, with the fully upgraded scheme, is sketched in Figure 2.1.

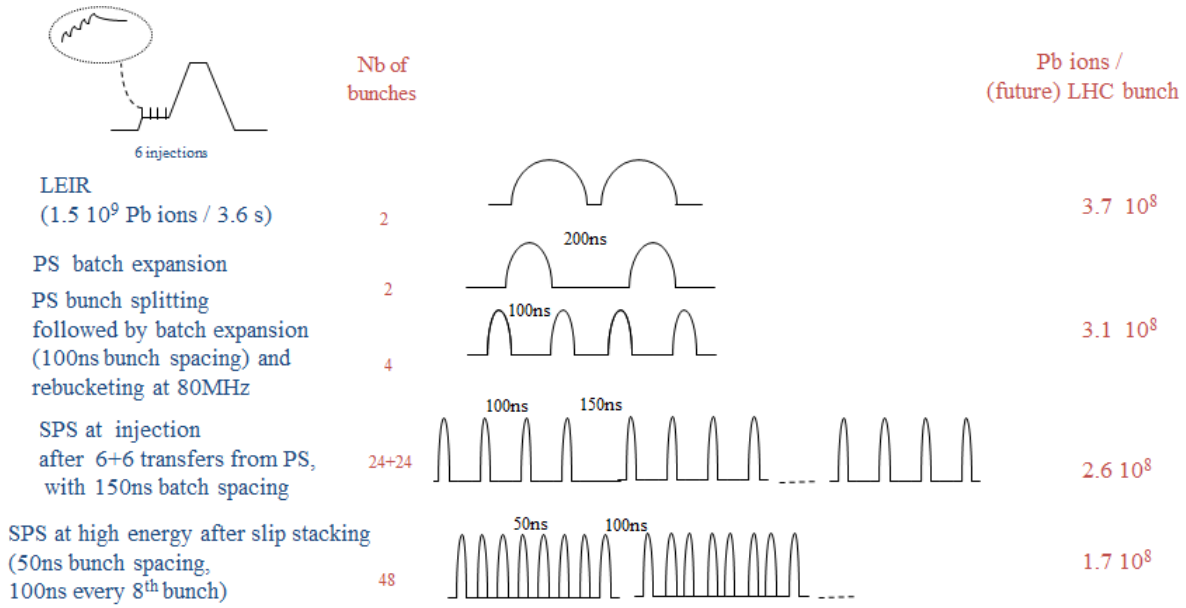

Figure 2.1 Baseline LIU-ions scheme.

2.2 LIU-ions baseline beam parameters

In this section, we discuss the potential LIU reach of the LHC ion injector chain, in the baseline LIU-ions upgrade scenario, as was presented in [4].
The definition of the beam parameters in the different accelerators of the ion injector chain is based on the following assumptions:

- 50 ns bunch spacing in LHC is requested as baseline. This relies on both bunch splitting in the PS and slip stacking in the SPS, since the usual RF gymnastics done for protons at 26 GeV in the PS cannot be done for ions, as their extraction energy is too close to transition energy. Consequently, since each LEIR bunch is split into two in the PS, the best performance of the injector complex relies on the increase of the intensity out of LEIR leading to SPS bunch intensities with optimal transmission.
- All the improvements upstream from LEIR (i.e. higher current from Linac3 and 100 ms injection rate) can lead to a 20% increase in the accumulated intensity with respect to the value achieved in 2015. Besides, we also make the further assumption that, even with this increased beam intensity in LEIR, the percentage of beam loss from the end of accumulation to extraction can be 20%. This value can be roughly extrapolated from the curve of the 2015 LEIR performance (see Chapter 3).
  The intensity limitation presently determining the LEIR performance is believed to be beam losses due to strong space charge. These losses mainly occur right after the beam is bunched and the high transmission of 80% can be achieved with the help of a better tailoring of the longitudinal beam parameters and/or resonance compensation, as it will be explained in further detail in Chapter 3. However, when larger intensity is accumulated in LEIR, the space charge limit might already appear in the coasting beam phase, which bounds the improvement achievable after all upgrades upstream from the LEIR injection. For this reason, we have assumed that the intensity increase in accumulated intensity in LEIR is 20%.
- The percentage beam losses in the transfer between LEIR and PS, as well as the losses along the PS cycle, are the same as in 2015 operation, i.e. both 8%. The bunches undergo a double

splitting at low energy in the PS, so that four bunches per extraction are sent to the SPS with 100 ns spacing between them.

- The percentage beam losses in the transfer between PS and SPS remain 16%, as was measured during 2015 operation. Part of these losses can be attributed to the presence of a stripping foil in this transfer line. Extensive studies were conducted in the past, which led to the design of a low-beta insertion for the LHC beams [7]. Further detailed studies of loss localization and optimization between losses and emittance growth at the foil traversal will be carried out in view of potentially reducing this figure.
- The spacing between subsequent injections into the SPS is 150 ns (see Chapter 6).
- Both the number of injections from the PS to the SPS and the LHC filling scheme have been optimized to yield the maximum total number of ions injected into the LHC, according to the procedure outlined in [5]. The result of this optimization procedure was 12 injections and a tightly packed LHC filling scheme with 1152 bunches, which however needs to be adapted to the experiments' requirements.
- The transmission in the SPS is assumed to be the same as in 2015 (see transmission curves in Chapter 6). This can be regarded slightly optimistic, as it assumes that the process of slip stacking will be lossless in the SPS.
- The transverse emittance evolution does not become worse up to the SPS injection, which means that it can still be assumed to be around 1 μm at the SPS injection. In the SPS, however, it is then allowed to blow up by 30% in future operation (down from the present 40-50%), due to the lower bunch charge.

Figure 2.2 shows the evolution of the Pb ion bunch intensity (in ions/bunch) along the injector chain after all the LIU upgrades, based on all the assumptions summarized above.

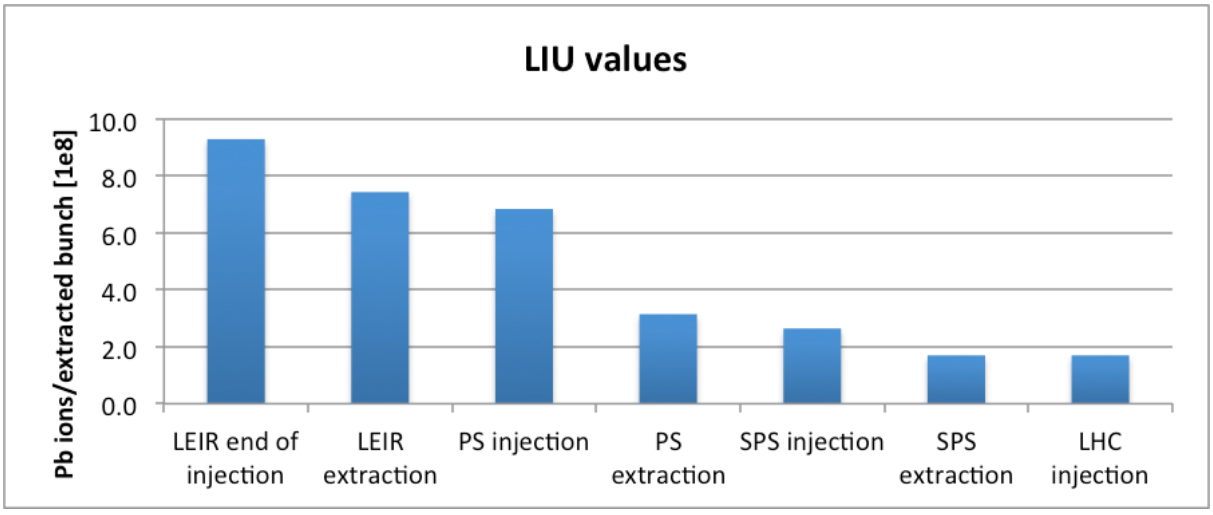

Figure 2.2 Bunch intensity at the different stages of the LHC ion injection chain.

Table 2.4 summarises the beam parameters at the different stages of the LHC injector chain (ion charge state and kinetic energy at each stage are also explicitly displayed), reporting values from the 2015 experience (Achieved 2015), for the post-LS2 LIU era (LIU-ions) as predicted using the assumptions outlined above, and for the HL-LHC desired scenario. For completeness, also the maximum number of bunches in LHC is indicated for the different scenarios.

Table 2.4 Beam parameters at the different stages of the LHC ion injector chain for the three scenarios: Achieved 2015, during the post-LS2 LIU era (LIU-ions) and from the HL-LHC request (HL-LHC).

	N_{ions}/bunch (10^8)	$\varepsilon_{x,y}$ (μm)	Bunches /injection	Bunch spacing (ns)	N_{ions}/bunch (10^8)	$\varepsilon_{x,y}$ (μm)	Bunches	Bunch spacing (ns)
LEIR	**Before RF capture (54^+, E_{kin}=0.0042 GeV/u)**				**Extraction (54^+, E_{kin}=0.0722 GeV/u)**			
Achieved	15.5	0.1, 0.4	coasting beam		6.0		2	354
LIU-ions	18.6				7.4		2	354
HL-LHC	29.5				11.8		2	354
PS	**Injection (54^+, E_{kin}=0.0722 GeV/u)**				**Extraction (54^+, E_{kin}=5.9 GeV/u)**			
Achieved	5.5		2	354	5.1	0.9, 0.8	2	100
LIU-ions	6.8		2	354	3.1	1.0	4	3x100
HL-LHC	10.9		2	354	5.0	1.0	4	3x100
SPS	**Injection (82^+, E_{kin}=5.9 GeV/u)**				**Extraction (82^+, E_{kin}=176.4 GeV/u)**			
Achieved	4.3	1.0, 0.9	2	100	2.2		24	11x(100+150)+100
LIU-ions	2.6	1.0	4	3x100	1.7	1.3	48	5x(7x50+100)+7x50
HL-LHC	4.2	1.0	4	3x100	2.1	1.3	48	47x50
LHC	**Injection (82^+, E_{kin}=176.4 GeV/u)**				Total number of bunches			
Achieved	2.2	1.5	24		518			
LIU-ions	1.7	1.3	48		1152			
HL-LHC	2.1	1.3	48		1248			

The yearly integrated luminosity estimated with the LIU beam parameters was also calculated following the method described in [1] and found to be about 2.5 nb^{-1}/year [6]. In particular, the estimate was made for 7 Z TeV operation and β*=0.5 m for each experiment, giving approximately equal luminosity sharing between the experiments (ALICE, ATLAS, CMS). The total number of bunches in collision was assumed to be 1056, lower than the theoretical maximum value of 1152, because it was calculated for a realistic filling pattern for physics, with the constraint of equal luminosity sharing, together with the delivery of a lower luminosity to LHCb. The LHC performance efficiency [8] assumed in the LIU scenario was also chosen to be 62%, which is the value achieved in 2015 and is significantly higher than that achieved for proton operation and assumed for the HL-LHC upgrade (i.e. 50%) [1].

In terms of integrated luminosity, the baseline LIU scheme has therefore the potential to provide 88% of the desired HL-LHC performance.

2.3 Project safety

2.3.1 Safety organisation

In accordance with the Safety Regulation SR-SO 'Responsibilities and organisational structure in matters of Safety at CERN', the Safety structure within the project is described in Figure 2.3.

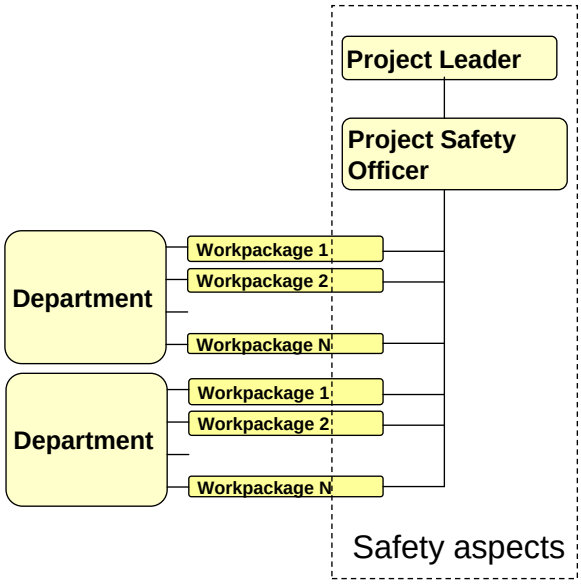

Figure 2.3 LIU Project Safety structure.

- The Project Leader is responsible for Safety in the Project.
- As defined in the General Safety Instruction GSI-SO-7, the Project Safety Officer (PSO) is appointed by the Project Leader to oversee and coordinate Safety aspects of the Project. The mandate is twofold:
    - The PSO verifies that Safety aspects have been correctly considered within the different work packages, that the solutions proposed are consistent with the general Safety policy of the Project and that the Safety measures are correctly applied by the different work packages.
    - The PSO verifies that there are no Safety issues arising at the interface between work packages. If this happens, he/she asks the relevant work packages to apply the appropriate measures.
- The work package Holders are responsible for proposing and applying the correct Safety measures for the work and equipment included in their work package. Because all work packages are contained within one Department, the Department of the work package is finally responsible for the Safety conditions of the work attributed to it by the Project.
- Territorial Safety is the responsibility of the Department where the work is done. The Department nominates Territorial Safety officers (TSO).
- The Safety Coordinators (EN-ACE):
    - Establish and update the work and safety coordination plan (PCTS in French for "*Plan de coordination des travaux et de la sécurité*").
    - Conduct the safety visits taking place before the start of the works (VIC in French for "*Visite d'Inspection Commune*").
- The Radiation Protection Group takes responsibility for all radiation protection aspects during the design, commissioning, operation and dismantling of the facility. In particular, the Radiation Protection Group takes responsibility for the results of all radiation protection studies (e.g. stray radiation, material activation, and air and water activation) and the derived radiation protection requirements for the facility.

2.3.2 Safety objectives

The program of upgrade of the injectors will ensure that the present level of Safety for the people and the environment is maintained during all project phases (simulations, design, prototyping, installation,

commissioning, operation and dismantling) and whenever possible or required, it will be improved. This will be demonstrated in the LIU Safety File.

In particular, the aim is to optimize the beam losses to favour technical solutions, which minimise the dose rates according to the ALARA principle (keep doses to persons as low as reasonably achievable) and minimize radioactive waste.

An example illustrating that Safety is integrated in the LIU-ions is the design, construction and installation of a clean beam dump for the beam extracted from LEIR.

Besides technical measures, organisational measures are also in place (non-exhaustive list):

- Work and dose planning (DIMR) aiming at optimization of the job to reduce the individual and collective doses;
- Use of TREC tool installed in the Buffer zones to trace potentially radioactive equipment;
- Correct management of the planning through the organisation of regular meetings ("LIU Installation and Planning meetings");
- Safety visits before the start of the works (VIC in French for "*Visite d'Inspection Commune*");
- Management of the interventions inside the accelerators using IMPACT. This web-based tool is used for inputting work declarations, planning, scheduling, preparing and coordinating all activities. The system also provides an approval process including radiation protection;
- Any modification to the project baseline, including Safety, is subject to an Engineering Change Request (ECR) process with an appropriate approval procedure. The impact of the modification on Safety is also assessed.

2.3.3 Safety documentation

2.3.3.1 Safety Packages (SP)

For the purpose of the Safety file, the LIU project is divided in Safety Packages (SP). A SP comprises a set of systems located in a same location under the responsibility of several groups. A SP does not change the fact that each group remains owner and responsible of their own Work Package (WP), which are covering their equipment or services. The LIU project includes 16 SPs. Three of them are devoted to the LIU-ions. The list is given in Table 2.5.

Table 2.5 List of LIU-ions Safety Packages.

		Safety Packages (SP)
		LIU new / upgraded equipment only
IONS	1	Linac3
	2	LEIR
	3	SPS RF

2.3.3.2 Safety Packages Coordinators (SPC)

A Safety Package Coordinator (SPC) is appointed for each SP. The SPC is acting as the technical link person for the corresponding SP.

His/her role is to ensure that the PSO and the editor of the safety files get the relevant information to produce the four parts of the SP safety files, with in particular:

- The brief description of the facility/system with focus on the Safety aspects;
- The preliminary list of hazards of the facility/system;
- The safety documents required to demonstrate the compliance of the facility/system with the Safety Rules and regulations as specified in the HSE Launch Safety Agreement;
- The safety-relevant procedures required to operate and maintain the facility/system safely.

2.3.3.3 HSE Launch Safety Agreement

The HSE Launch Safety Agreement (LSA) covering the conventional safety aspects are/will be produced at the level of the SPs.

For each SP, a launch safety discussion take place with the SPC, the Machine Activity Leader, the Project Safety Officer (PSO) and the correspondent from the HSE Unit. After the launch safety discussion, the HSE correspondent releases the Launch Safety Agreement that provides the following information:

- Description of the SP systems/processes;
- Preliminary identification of the safety hazards and risks;
- Identification of the CERN Safety rules and Host State regulations applicable to the systems/processes;
- Tailored Safety advice on hazard control measures;
- List of Safety checks (including Safety checks required to grant Safety clearance) on the relevant systems/processes that shall be carried out by the HSE Unit during the SP life cycle;
- Minimal contents of the SP Safety File needed to meet the Safety requirements
- The LSA may be reviewed and updated during the different phases of the systems/sub-system's life-cycle. Any changes to the safety requirements will be integrated through the ECR process.

2.3.3.4 LIU Safety File

The Safety File for the LIU project will be established and maintained during the project life cycle. It will consist of the collection of the approved Safety Files of each SP. The structure and contents of each part of a SP Safety File are given in the templates available in EDMS [9], which follow the "Quality Procedure for Safety Documentation Management" [10].

The PSO ensures that the LIU Safety File is kept up-to-date, available in the EDMS structure of the LIU project [11] and provided to the HSE Unit for granting safety clearance.

Once the facility/system of a SP is in operation, the corresponding Safety File will become part of the Safety File of the corresponding machine and attached to the CERN Safety File structure in EDMS [12].

2.4 Project timeline

All relevant LIU related studies (both machine and simulation), many of which extensively started during Run 1, need to be carried out during Run 2 and finished by the beginning of Long Shutdown 2 (LS2). These studies are crucial for both the optimisation of the ion beams and to provide all the necessary information to launch possible corrections to the baseline scenario, compatible with the cost and timelines of the project, and define the best operational scenarios for post-LS2. Besides, during this time, some of the LIU equipment will have to be designed and procured (e.g. LEIR dump, hardware for the new LLRF of the 200 MHz cavities in the SPS). For the ions, only few of the LIU hardware modifications and installations will have to wait until LS2 (e.g. Linac3 hall ventilation system, LBS line, LLRF for slip stacking in SPS), while many activities are advanced to the previous Year-End Technical Stops (e.g. the Linac3 hardware modifications to enable 10 Hz injection rate into LEIR, LEIR beam dump). Following the general operation schedule until 2021, LS2 will start at the beginning of 2019 for all machines and the injector chain will resume operation after LS2 in the second half of 2020.

Linac3, LEIR, PS and SPS will be taking ion beams in a cascade from the third or fourth quarter of 2020 (Linac3) until the second quarter of 2021 (SPS). A first schedule of LS2 (including activities foreseen to take place during previous YETS's) has been prepared and was presented at the Chamonix 2016 Workshop [13]. The final schedule will still be refined in the coming years, while an optimum use of the access time during the machine stops before LS2 is being performed and the work plan is gradually finalized, including the information on available resources.

The commissioning of the final LIU ion beams, with parameters outlined in the previous section, will have to be carried out during the 2021 run in order to be able to deliver beams to LHC already for the first Pb-Pb run, scheduled to take place at the end of 2021. This highlights an important difference between the preparation of the post-LS2 proton and ion beams: while the proton beams will be prepared and tuned throughout Run 3, and corrective actions taking place during the Technical Stops between LS2 and LS3, the Pb ion beams will have a short commissioning time, to be ready for physics production at the end of 2021.

2.5 References

[1] J.M. Jowett, *HL-LHC heavy-ion beam parameters at LHC injection*, EDMS 1525065 (2015).

[2] The ALICE Collaboration, *Upgrade of the Inner Tracking System Conceptual Design Report*, CERN-LHCC-2012-013 (LHCC-P-005), September 2012 and ALICE LOI CERN-LHCC-2012-012.

[3] H. Bartosik, A. Huschauer and G. Rumolo, *Preliminary analysis of 2015 ion beams*, in LIU Beam Parameter Working Group meeting, 8 January 2016, CERN (2016).

[4] H. Bartosik, B. Goddard and G. Rumolo, *LIU ion beam parameters specification*, in LIU-ions overall status and outlook meeting, 18 January 2016, CERN (2016).

[5] M. Schaumann, *Heavy-ion performance of the LHC and future colliders*, CERN-THESIS-2015-195 .

[6] H. Bartosik et al, *LIU beam parameters specifications for ions at the exit of the SPS*, EDMS 1581381 (2016).

[7] G. Arduini et al., *Lead Ion Beam Emittance and Transmission Studies in the PS-SPS Complex at CERN*, THP017G in Proc. of EPAC 1996, 10-14 June 1996, Sitges, Spain (1996)

[8] G. Arduini et al, *Beam parameters at LHC Injection*, CERN-ACC-2014-0006 (2014).

[9] Templates for the SP Safety Files of LIU, https://edms.cern.ch/project/LIU-000012

[10] P. Bonnal *et al*., Quality Management Procedure – Safety Files Management, EDMS 1177755

[11] EDMS structure for the Safety File of LIU, https://edms.cern.ch/project/LIU-000407

[12] CERN Safety Files structure in EDMS, https://edms.cern.ch/project/CERN-0000092982

[13] J. Coupard, *LIU Activities during LS2, highlight of changes with respect to last year*, in LHC Performance Workshop – Chamonix 2016, 25-28 January 2016, Chamonix, France (2016).

3 Pb-ion source and Linac3

3.1 Introduction and present operational performance

The heavy ions for the CERN ion accelerator chain are delivered from Linac3 (see Figure 3.1) and the GTS-LHC ion source [1]. Isotopically enriched ^{208}Pb with a purity of 99.6% is used to create the Pb-ion beam. After the separation of the charge states, Pb^{29+} is accelerated in the Linac3 and sent through a stripper foil. From all resulting charge states, Pb^{54+} ions are selected by the filter line before sending the beam to LEIR.

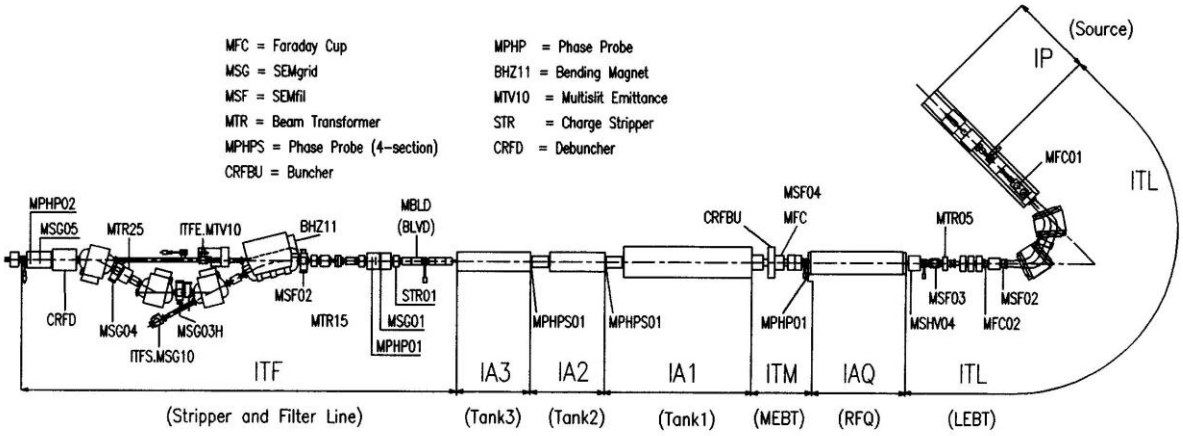

Figure 3.1 Layout of Linac3.

Up to now, the following record values have been achieved: 215 µA of Pb^{27+} after the charge state separation in the spectrometer (measured with the Faraday Cup FC2) and 31 µA of Pb^{54+} at the end of the Linac3 (ITF.BCT25, with 120-130 µA of Pb^{29+} in FC3). However, both values were not achieved at the same time, neither is it possible to produce them for long term operation, or even on demand. Maximizing the ion current at the output of the spectrometer very often leads to a poor transmission in the rest of the Linac3. This issue is part of an ongoing study. For routine operation, 100 – 120 µA of Pb^{29+} out of the RFQ (measured with the Faraday Cup FC3) and 20-25 µA of Pb^{54+} at the end of the Linac3 (ITF.BCT25) are available. The current at the end of the Linac3 corresponds to less than 50 % of the design value.

All modifications to the Linac3 complex described here are within the scope of the LIU-ions project, unless they are specifically noted to be financed by other projects (e.g. CONSolidation project) or as part of operation. The main upgrades consist of modifications on the LEBT and enabling Linac3 to inject into LEIR at the increased rate of 10 Hz. A detailed description of the planned modifications of all systems concerned is given in the following sections.

3.2 Ion source and oven test stand

The GTS-LHC ion source is an electron cyclotron resonance ion source (ECRIS) [2]. It is running in the so called afterglow mode, using the 14.5 GHz microwave plasma heating with 10 Hz repetition rate, 50 % duty cycle, where at the end of each heating pulse, a burst of approximately 1 ms in length of highly charged ions is emitted from the source. A pulse length of 200 µs is used in the Linac3 with a repetition rate of up to 5 Hz for LEIR filling.

Two ovens are available during operation for the evaporation of the solid lead into the plasma. There are around 1.5 g of lead in each oven. The consumption is roughly 2 mg/h, but not all the lead in the sample can be used. The first oven can supply lead for around two weeks, while the second one only for another week, because it sees some plasma during the first two weeks. But there is a flexibility of some additional days after the three weeks.

At the end of its lifetime, the tip of the oven is usually blocked (see Figure 3.2). An oven refill takes around 8 hours from beam to beam, with the source requiring regular tuning for the next 24 hours. This is down time for the whole Pb-ion accelerator chain.

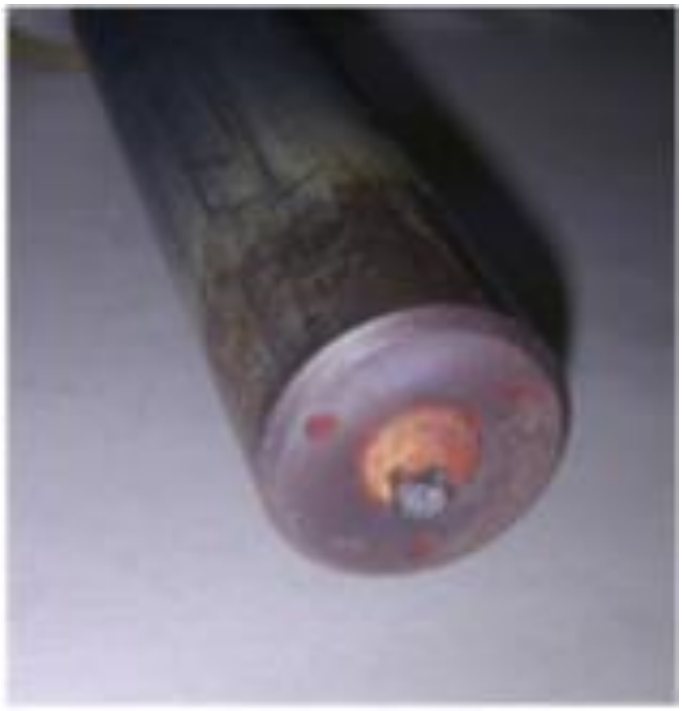

Figure 3.2 Tip of an oven after two weeks of operation.

An oven test stand is foreseen to study the oven (temperature distribution, relation between oven power and the evaporation of lead). The result of these studies may help to improve the oven and source tuning to get a more stable beam in the long term. In addition, a redesign of the oven is not excluded, but would require a redesign of the whole source injection side (due to the present constraints).

Most of the equipment for the test stand has been purchased using operation budget, and the LIU budget will pay for instrumentation for the lead evaporation rates as well as oven consumable pieces and canes (holding and connection rods).

3.3 Low Energy Beam Transport (LEBT)

The present Low Energy Beam Transport (LEBT) is quite long and has only a very limited number of elements for beam diagnostics. A study campaign was launched in 2014/15 to understand and reproduce the present behaviour of the line with currently available simulation tools (IBSimu [3] and PATH [4]) and benchmark the simulation results with measurements. Scope of the exercise was to determine the bottlenecks in the present line and find possible solutions to overcome them with a partial redesign of the line.

Comprehensive studies of the beam formation at the GTS-LHC ion source have been carried out with the code IBSimu, and the resulting beam distributions handed over at an agreed extraction plane for further tracking through the LEBT with PATH. Several issues limiting the machine performance have been identified through these studies.

As illustrated in Figure 3.3, the beam extracted from the ECR source operated in afterglow mode has a very strong divergence, causing significant beam collimation on the first element encountered downstream (the magnetic solenoid ITL.SOL01), due to the present aperture restrictions of the vacuum chamber (65 mm diameter). PATH simulations show that the transmission of $^{208}Pb^{29+}$ beam through this region and the following spectrometer dipoles to the slit varies between 50 and 60%. This result compares well to beam transmission measurements during operation: typical readings on the first available transformer at the end of the LEBT (ITL.BCT05) show an average current of around 150 μA in good operation, to be compared to an estimated beam current at source extraction of approximately 5 mA (5% of which is the $^{208}Pb^{29+}$ component).

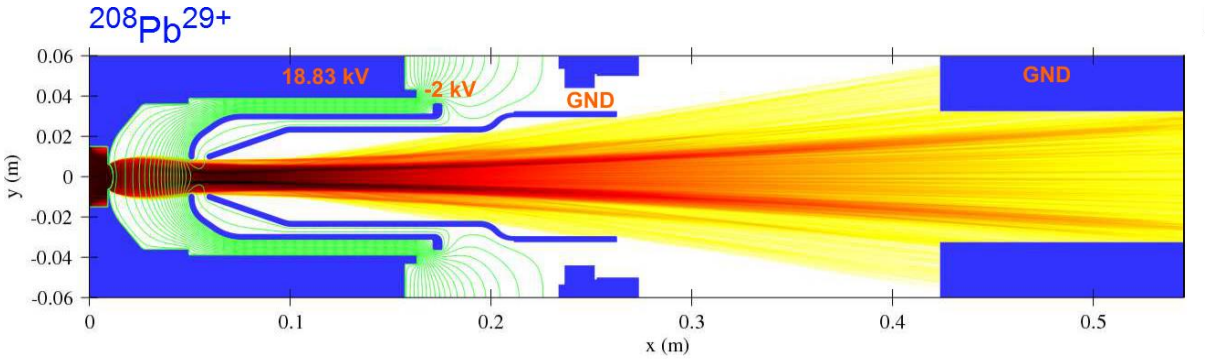

Figure 3.3 Extraction of the ion beam from the Linac3 GTS ion source, simulations performed with IBSimu. Blue: Electrodes; Green: Equipotential lines; Yellow/Red: Ion density.

Together with the large beam divergence, the other main finding of these studies is that the beam transverse emittance also plays a relevant role. Simulation results with IBSimu show that already at the GTS-LHC source extraction (see Figure 3.4) the beam emittance exceeds by nearly a factor of 2 the geometric acceptance of the RFQ installed just downstream of the LEBT (360 mm mrad vs 200 mm mrad, in 5rms un-normalised values). Direct implication of this, is that only about 56% of the lead ions produced by the source can eventually fit in and be accelerated by the RFQ, no matter how good is the transmission efficiency in the LEBT. The initial beam collimation at the source output may have in these conditions rather worked as beneficial effect towards an overall beam emittance reduction and transmission improvement.

This result was confirmed by indirect emittance measurements via a quadrupole scan technique carried out using the magnets triplet at the end of the LEBT section. These yielded rms normalized emittance values in the order of 0.2-0.25 mm mrad for the vertical and horizontal plane respectively.

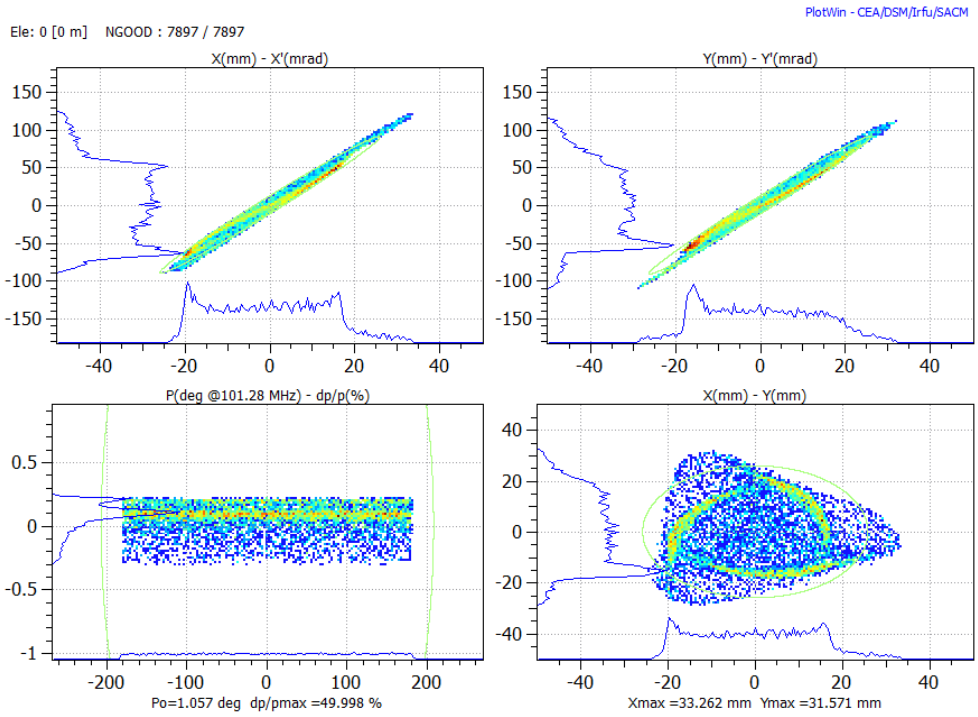

Figure 3.4 Simulated $^{208}Pb^{29+}$ beam distribution at the GTS-LHC source extraction. From top left clock-wise: horizontal, vertical and longitudinal phase space, and transverse cross-sectional cut x-y.

Hardware modifications to the GTS-LHC source extraction and initial LEBT regions have been planned in the framework of the LIU project to overcome or at least mitigate these performance limitations. The first one consists in an aperture increase from 65 to 100 mm (diameter value) of the beam pipe connecting the source extraction pumping chamber to the ITL.SOL01 solenoid, which should reduce current beam losses in the region. The second is the addition of a focusing electrostatic Einzel lens [5] (see Figure 3.5) inside the source pumping chamber, adjacent to the existing extraction electrodes. The Einzel lens should allow more control over the beam divergence and decouple the beam transport and matching through the extraction region from the ion source tuning and optimization of the beam production. The Einzel lens can be operated in accelerating or decelerating mode with absolute voltages up to 20 kV. This should also potentially bring more flexibility in operation with different ion species.

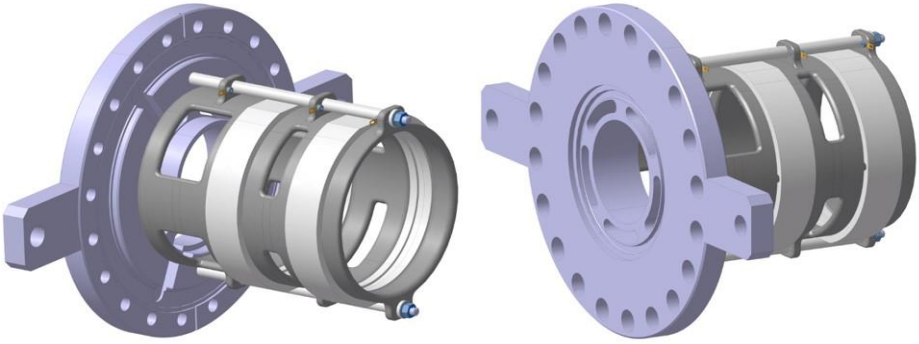

Figure 3.5 Einzel lens mechanical design.

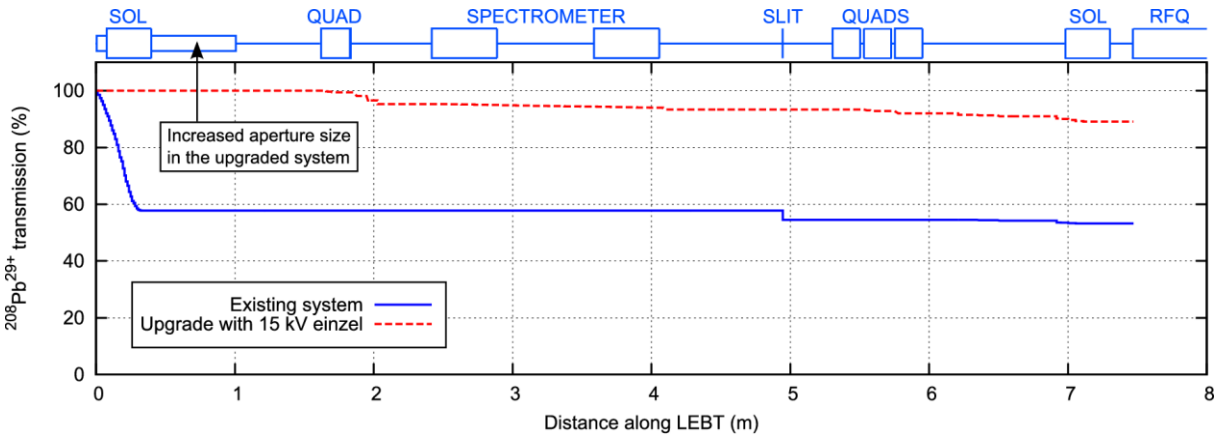

Figure 3.6 Transmission of $^{208}Pb^{29+}$ through the LEBT to the RFQ entrance with the existing (blue line) and upgraded (red) extraction system with 15kV applied Einzel lens voltage.

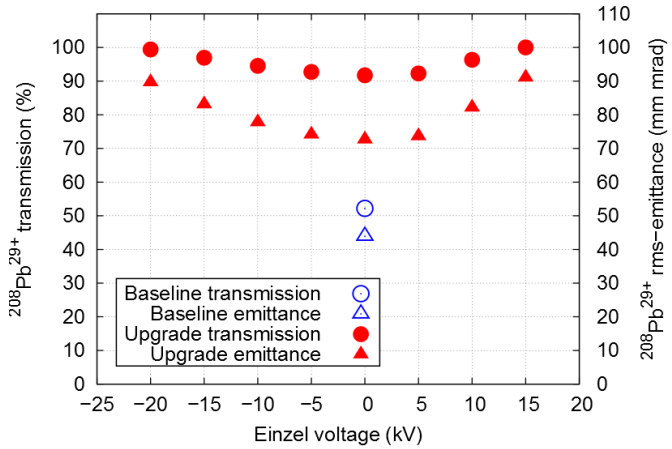

Figure 3.7 Comparison of Pb transmission through the LEBT between the existing (baseline) and upgraded systems for different Einzel lens voltage values. The $^{208}Pb^{29+}$ emittance, at the solenoid exit, is here normalised to the baseline value (~50 mm mrad rms.).

Both upgrades have been installed at Linac3 during the YETS 2015/16 and are being commissioned at restart of operations in February 2016. Simulations of the beam extraction and transport through the LEBT with these upgrades have been carried out with IBSimu and PATH, and results are shown in Figure 3.6. The beam transmission through the LEBT can be expected to increase up to 90% for optimized values of the first solenoid, even if the Einzel lens voltage is switched off, compared to only 50-60% for the present system. No significant effect is however predicted on the beam transverse emittance at the GTS-LHC source extraction. As shown here in Figure 3.7 (values taken at the solenoid exit and normalized to the current baseline value of ~50 mm mrad rms), the beam transverse emittance is in fact expected to increase, as a result of the different matching in the LEBT and beam loss mitigation in this section. Hence the higher beam transmission we expect to achieve in the LEBT will most likely not propagate entirely all the way through the RFQ, due to the shown acceptance bottleneck. An overall gain of up to 20% in the beam intensity delivered at the end of Linac3 can be expected as a combined result of these upgrades.

Predictions from simulations will be verified during the startup of operations in the first quarter of 2016: a systematic campaign of recommissioning of the low-energy part of Linac3 is being planned, which will also benefit from diagnostics improvements and the re-installation of a pepper-pot based emittance measurement system, downstream of the spectrometer magnets.

Further source development options are being explored in parallel (outside of the scope of the LIU project baseline) to investigate possible solutions to the emittance reduction problem at the source extraction, as well as to build in more flexibility in the beam production from the source.

3.4 Linac3 modifications for 100 ms operation

The production of the nominal LHC beam is presently based on 7 injections from Linac3 into LEIR. To increase the accumulated intensity in LEIR, the time in between injections will be decreased from the present 200 ms to 100 ms, so that up to 13 injections can be accommodated on the injection plateau of the 3.6 s cycle. This scenario leads to an average Linac3 pulsing rate for LEIR injection of 3.6 Hz (i.e. 13 injections during a 3.6 s cycle). In addition to this, the already existing requirement of 5 Hz continuous injection rate for LEIR scrubbing should be maintained [6].

The Linac3 source runs already at 10 Hz continuously and the RF system adds additional pulses while the LEIR ramp takes place (the RF pulses are spaced by approximately 1.5 s) in order to allow the cavity tuning to be maintained. Although Linac3 was initially specified for operation at 10 Hz, it was never tested and was never used operationally during the more than 20 year existence of the Linac3. Therefore an analysis has been made on the Linac3 systems, and as described in more detail below, hardware modifications are needed for some systems in order to allow for 100 ms spaced pulses to LEIR.

The hardware changes (apart from the hall ventilation) have been advanced to the YETS2015-16, so that higher repetition rate can be tested at LEIR during the 2016 lead ion run.

3.4.1 RF Systems

The RF systems are capable of supplying 200 μs long pulses (flat top regulated) with 100 ms spacing. Attention needs to be paid to the air-flow in some amplifiers, but no upgrade is needed. The ramping cavity, the debuncher cavity amplifiers and controls are also able to operate at 100 ms spacing (it is not necessary to change the RF function between 100 ms injections, the same function is valid for all injections on one LEIR cycle).

3.4.2 Stripper

The stripper consists of 75 $\mu g/cm^2$ carbon foils (non-annealed) inserted in the ITF line of Linac3 just in front of the ramping cavity. The increase in injection rate from Linac3 to LEIR will increase the average Linac repetition rate for LHC beam production from 1.9 Hz to 3.6 Hz and this will shorten the lifetime of the foils. It has always been possible, and will remain possible, to run with up to 5 Hz quasi-continuous injections into LEIR for scrubbing. This was done for the last time in 2009.

The foil holding system has been consolidated during LS1, and is able to hold up to 4 foils per actuator with 4 actuators installed. Each actuator system can be independently retracted from the beam line and have its frame replenished with new foils. Only a short (approximately 4 hours) beam stop is required for personnel to access the area, after which the pumping of the system can be done with beam still operational. With this system in place, it should be possible to cope with stripper foil lifetimes down to one week. If after testing the 100 ms injection rate the lifetime is found to be so short, tests could be made with alternative foils such as for example Diamond Like Carbon, which could offer better lifetime.

3.4.3 Magnets and magnet interlocks

The vast majority of the magnets in the transfer lines from Linac3 to LEIR are run in DC mode. Only ten quadrupoles in the ITF, ITH and ITE lines, as well as the trajectory correction dipoles are pulsed. The requirement to run with 100 ms bursts at an average repetition rate of up to 5 Hz is feasible: the rms current has been analysed to verify that the magnets can work in this regime continuously. Furthermore,

measurements in 2014 [7] proved that the temperature levels reached are acceptable (although much closer to the limits than were found for the nominal Pb-ion beam production regime for LHC).

In order to be consistent with the policy of having all magnets equipped with thermal interlocks, and to mitigate the effect of running several pulsed magnets closer to their thermal limit, these magnets have been equipped with thermo-switches and connected to the existing Warm Interlocking Systems (WICs) of Linac3 and LEIR during the 2015-16 YETS.

3.4.4 Power Converters

For the power converters of quadrupole magnets, the following option has been adopted to allow the 2016 operation with 100 ms spaced pulses for machine studies:

- The present MAXIDISCAP power converters were modified during the 2015/16 YETS to include new capacitor charging supplies. The associated electronic control crates will stay in place with MIL1553 control.
- At a later date to be defined (2017/18 YETS or LS2), the electronic crates will be replaced in order to adopt FGC3 control and digital current regulation. Some modifications will also be implemented on the power converter part to cope with these changes on the electronics side.

Considering that the hall ventilation system will be implemented later, the use of 100 ms repetition rate will be limited such as to stay within present hall temperature limits, which is acceptable up to LS2 as the higher injection rate will not be used for LHC filling but only during machine studies.

Concerning the power converters for pulsed dipole magnets, it has been decided to reduce their output current limits from ±20 A to ±10 A in order to allow the operation with 100 ms repetition rate using the existing converters. This is not expected to impose a limitation for operation, since the correction of the transfer line trajectory did not require output currents of more than 8 A so far. Some minor modifications are required on the regulation system; they were implemented during the 2015/16 YETS, at the same time as the quadrupole power converters upgrade.

3.4.5 Controls

The Linac3 will still use the 1.2 s basic period as the control setting and acquisition cycle. Multiple triggering within a basic period is used to initiate multiple injections. Beam intensity instruments need to be able to measure the beam intensity for shots at 100 ms spacing, and the OASIS distributed oscilloscope already triggers, acquires and displays at 100 ms spacing.

3.4.6 Cooling and Ventilation

The cooling and ventilation of the Linac3 building is dominated by the average power load. Linac3 already had an operational requirement to run at 5 Hz repetition rate for LEIR scrubbing. Analysis of the scrubbing periods in the past has shown that operation was often interrupted due to higher temperatures in the Linac3 hall, and the source had to be run at lower magnet settings (leading to lower intensity).

A dedicated test was made in 2014 [8], which showed that the ventilation system is at full capacity for today's standard operation, and pulsing at 5 Hz causes an increase in air temperature that the ventilation system is not able to compensate (even if this additional heat load generated by going from 1 Hz to 5 Hz operation is only a few kW).

The ventilation system in particular is reaching the end of its lifetime and should be renovated during LS2, and the renovation must be designed with sufficient margin for operation at this maximum power load, in particular during the summer months. The budget for this work is approved by the CONSolidation project. The consolidation of the ventilation system has an impact on the civil engineering requiring the eradication of asbestos from the Linac3 building. The removal of asbestos will

require approximately 4 months, during which other works in the Linac3 building must be avoided. Afterwards, the ventilation system work can begin, which will take approximately 8 months. During this time only a temporary cooling system can be put in place to cool power systems for vacuum pumping.

It is not possible to make the renovation of the cooling systems before LS2. However, it will be possible to test the 100 ms spaced injections in LEIR with a restricted duty cycle, i.e. with a sufficient number of LEIR cycles with a low number of injections in the super cycle.

3.4.7 Radio Protection

Due to the low beam intensity and energy, the Linac3 hall is accessible during beam operation, with the main sources of radiation being x-rays from the IH structure and the source. Even though the Linac3 pulse spacing will be decreased to 100 ms, the source already runs at this spacing, and the RF will not be operated with an average rate higher than 5 Hz. Under these assumptions, and that only Pb ions are considered part of the LIU-ions project, the present radio protection measures in place are already sufficient, i.e.,

- The hall is declared a Simple Controlled Radiation Area.
- Radiation levels are surveyed by the RAMSES radiation monitoring system, which produces audible alarms in the Linac3 hall if the predefined alarm thresholds are exceeded.
- The presently installed shielding around the RF structures and the source is sufficient.
- Access to higher radiation zones (next to the beam line) is prevented during operation by simple barriers with warning panels.
- The average repetition rate of the RF system is limited by a simple pulse counting electronics, which allows the RF to pulse only 150 times within 30 seconds.

3.5 LBS Spectrometer Line

The Linac3 beam energy and energy spread can be measured in the LBS line using a classical spectrometer (input slit, spectrometer magnet and SEM-grid beam profile measurement). The LBS line is inside the PS tunnel and up to LS2 is shared with the Linac2 proton beam (see Figure 3.8). The line was originally foreseen to be replaced by the Linac4 project with a new version, using the same basic principles. However, due to the additional complexity of dumping the 160 MeV H^- beam in the zone, the Linac4 beam measurements will be performed with a bunch reconstruction technique that does not require the LBS line. Therefore the line is left for use with ions only.

As major renovation of this line was on hold due to its impending replacement, it now needs renovation. This work will take place in LS2, when there will anyway be major installations foreseen in the same area and will be the best period to remove the main spectrometer of the LBS line for any exchange or renovation.

Assessing the LBS line in its present position has led to the following conclusions:

- Power Converters: The power converters of the bending magnets LTB.BHZ40 and the present LBS.BVT10 are covered by Linac4 items. They are compatible with operating LTB.BHZ40 at 2 Hz and LBS.BVT10 in DC mode for ions (including a cycling procedure controlled by an application, that increases the reproducibility of the magnetic field).
- Magnet: The spectrometer magnet of the LBS line will be replaced with an equivalent magnet from the LTL line in Linac2 (which will no longer be needed). These magnets will be qualified by the magnet group before one of them is moved to the LBS line. The tooling for removal and installation of these magnets is in the LIU budget.

- Vacuum Equipment: The vacuum pumping of the LBS for ions in its present location requires a renovated pumping group that is already in the consolidation budget. The vacuum chamber of the LBS.BVT10, if necessary, can be replaced in the frame of the LIU project.
- Beam Instruments: All the SEM-grids in the LTB and LBS lines are already upgraded to new electronics. Beam Current Transformers in the LTB and LBS lines need to be made available for ion measurements, and their signals integrated into the control system. The controls for instruments need to work correctly with Linac3 and Linac4.
- Slits: The controls of the slits have already been renovated and do meet the requirements for ion operation. However their specification was driven by proton operation and the mechanics could be simplified in the long term under the consolidation programme, even though not necessary.
- Cooling and Ventilation: The LBS line has demineralised water cooling for the LBS.BVT10 magnet and the slits. The cooling requirements will remain in general the same, but the supply of water should be clarified in view of Linac4's connection to the PS complex.
- Cabling: The cabling already installed needs to be verified for its long term reliability.
- Controls: The equipment in the LBS line will be attached to Linac3, while the equipment in the common LTB line would have to be controlled in a way that allows the settings and timings to be mastered from Linac4 or Linac3 depending on the cycle. Beam instrumentation controls hardware is already renovated to be compatible with this approach (software still needs completing and testing) whereas for the power convertors of magnets in the common LTB line, FGC3 controls hardware needs to be installed (a request has been made to the CONSolidation project).

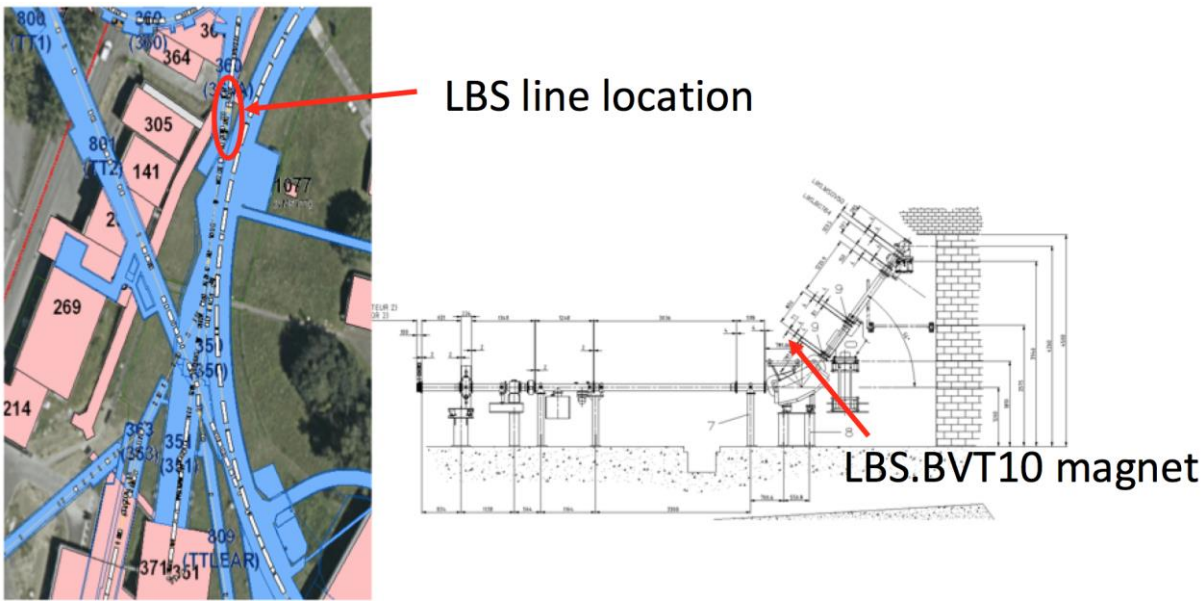

Figure 3.8 Location of the LBS line and the spectrometer magnet LBS.BVT10.

Using the LBS (and LBE) line means sending the ions in the direction of the PSB and there is a small possibility of the ions hitting the PSB injection foil. An estimate of the heat deposition per ion pulse is a factor 3 lower than the deposition from an H^- beam pulse [9]. This estimate was made assuming that the beam impact area of ions on the foil is by a factor 2.35 larger than that of the H^- beam, and that all the ions are transported up to the foil (very unlikely as the transfer line magnets on the BI (Booster Injection) section of the transfer line will not be set up for beam transport). This leads to the conclusion

that no specific additional measures are needed to avoid sending the ion beam onto the PSB injection foil.

Beside LBS, other beam diagnostics tools located in Linac3 (Figure 3.1) or transfer lines to LEIR (downstream from ITF: ITH-ITE-ETL-EI) will also be upgraded during the (E)YETS's, or simple technical stops, before LS2. In particular, some new Faraday cups to measure the beam intensity are planned to be installed in ITL and ITF, while the existing one in ITM will be modified in order to improve its accuracy. The SEM grids to measure the beam transverse profile will also be renovated. The wires will be changed to bands for the grids in ITF and ITH, while a new design will be implemented for those in ITL-ITM. The electronics of the SEM grids in ETL will also be changed to allow for a better measurement of the injected and extracted beam.

3.6 References

[1] D. Manglunki, M.E. Angoletta, P. Baudrenghien, G. Bellodi, A. Blas, T. Bohl, et al, *Ions for LHC: performance of the injector chain*, CERN-ATS-2011-050 (2011).

[2] L. Dumas, C.E. Hill, D. Hitz, D. Küchler, C. Mastrostefano, M. O'Neil, et al, *Operation of the GTS-LHC Source for the Hadron Injector at CERN*, LHC Project Report 985, (2007).

[3] T. Kalvas, et. al, *IBSIMU: A three-dimensional simulation software for charged particle optics*, Rev. Sci. Instrum. 81, 02B703, (2010).

[4] A. Perrin, J.F. Amand, T. Mutze, J.B. Lallement, and S. Lanzone, *TRAVEL v4.07: User Manual*, CERN, April 2007.

[5] H. Liebl, Applied Charged Particle Optics (Springer, Berlin, 2008), chapter 1, p.39.

[6] LHC Design Report, Volume III The LHC Injector Chain, Editors: M. Benedikt, P. Collier, V. Mertens, J. Poole, K. Schindl, CERN 2004-003, (2004).

[7] D. Bodart, 5 Hz Magnet Tests at Linac3, private communication.

[8] S. Deleval, Linac3 Ventilation Test at 5 Hz Operation Rate, private communication.

[9] V. Vlachoudis, private communication.

4 LEIR

The Low Energy Ion Ring LEIR has accumulated, cooled and stacked ion beams of oxygen (O^{4+}), lead (Pb^{54+}) and argon (Ar^{11+}). The number of lead ions injected into LEIR could be increased during several machine development studies (MDs) in late 2012 and early 2013. Total intensities of up to $1.8x10^9$ lead ions could be achieved during the coasting beam phase. However, large losses were observed during and after the RF-capture limiting the intensity of the two bunches at extraction to a maximum of $5.8x10^8$ ions per bunch. Intense machine studies at the end of 2015 showed strong indications that the losses are caused by direct space charge. After a first attempt of empirically compensating third order resonances using the existing harmonic sextupole correctors, the maximum intensity of the two bunches at extraction could be increased to the record level of $6.5x10^8$ ions per bunch.

In the LIU era, LEIR is requested to deliver two bunches containing $7.4x10^8$ ions, which is 65% more than the $4.5x10^8$ originally required for the LHC project, and 25% above the stable operating intensity of $6.0x10^8$ achieved in the last Pb^{54+} ion run in 2015. Reaching this intensity relies on the following improvements and optimizations

- Increase the injection rate from Linac3 into LEIR from 5 to 10 Hz ("*100 ms operation*");
- Reduction of the direct space charge tune spread through longer bunches;
- Optimization of the resonance compensation scheme, or operating the machine at a working point further away from critical resonances.

4.1 LEIR cycle

The LEIR cycle presently used for filling the LHC with lead ion beams has a length of 3.6 s and the injection plateau presently accommodates 7 injection pulses from Linac3, which are spaced by 200 ms (5 Hz injection rate). Figure 4.1 shows the "Nominal" LEIR cycle with the typical intensity achieved in 2015.

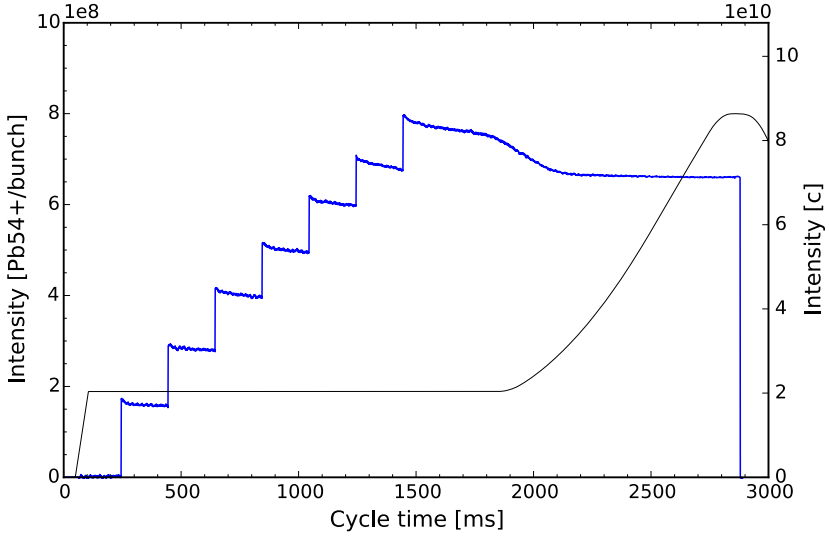

Figure 4.1 "Nominal" LEIR cycle in 2015.

LEIR features a multi-turn injection with simultaneous stacking in momentum and in both transverse phase spaces. The nominal working point (Qx, Qy) = (1.82, 2.72) was chosen to optimize the injection efficiency [1]. The phase space volume of the stack is reduced in between injections by electron cooling.

Before acceleration, the coasting beam is captured in h=2+4 and two bunches are extracted towards the PS.

4.2 Characterization of LEIR performance limitations

In 2015, an intense program of machines studies was devoted to the understanding of the LEIR intensity limitations, with focus on the losses occurring during and after RF capture. These studies indicate that the losses result from the enhanced direct space charge tune shift for bunched beams, which pushes individual particles onto betatron resonances. This conclusion is based on the following experimental observations:

Dependence of losses on longitudinal line charge density: Enhanced losses after RF capture are observed in case the peak line charge density exceeds a certain level. Figure 4.2 shows a comparison of the intensity evolution along the LEIR cycle for three different longitudinal phase space distributions. In all three cases, the RF voltage functions were programmed such as to iso-adiabatically capture the coasting beam. The losses clearly increase with the peak line charge density, i.e. with increasing incoherent tune spread due to direct space charge.

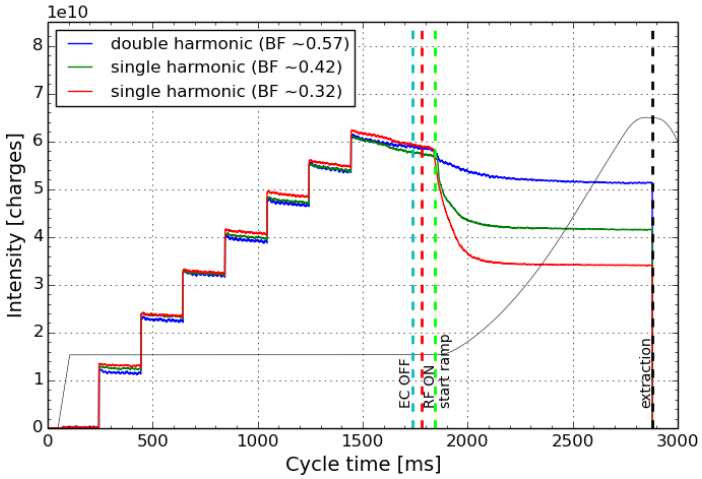

Figure 4.2 Comparison of losses for different longitudinal line densities. Vertical lines indicate the moments when the e-cooler is switched off, the RF is switched on, the start of the ramp and beam extraction. The bunching factor (BF) for each case is indicated in the legend.

Losses on flat bottom with bunched beam: A special LEIR cycle with 4.8 s total length was used in order to check the behavior of the bunched beam after RF capture on the injection plateau. Multiple injections from Linac3 were accumulated to reach comparable intensities as with the "Nominal" LEIR cycle. RF capture took place about 300 ms before acceleration and Figure 4.3 shows the intensity evolution along the cycle for the case of single harmonic RF capture. The loss rate was found to significantly increase soon after the beam is bunched. These losses occur already on the injection plateau and practically no change of the loss rate is observed during the first ~200 ms of the ramp.

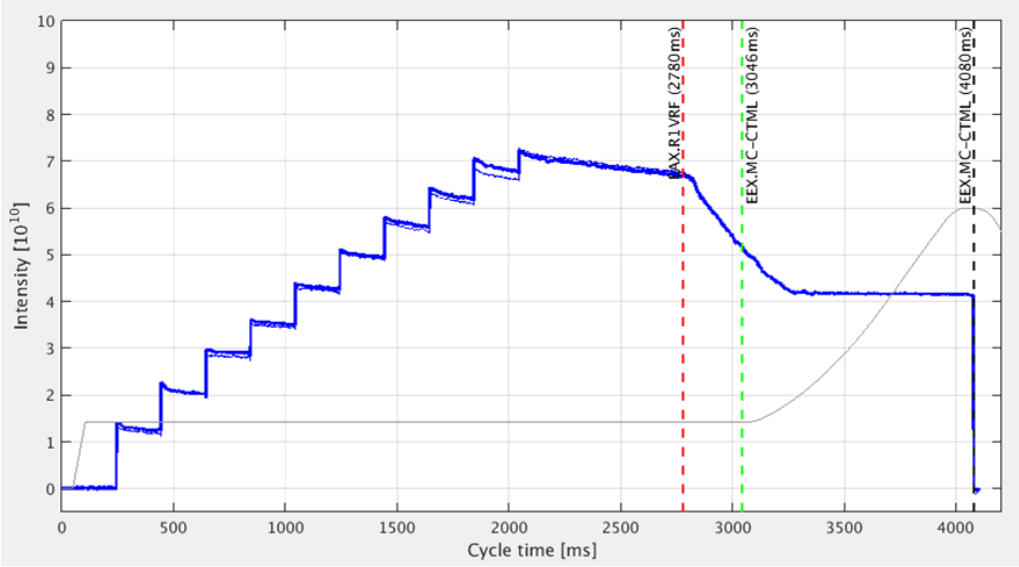

Figure 4.3 Losses on the injection plateau with advanced RF capture (indicated by the red vertical line).

Direct space charge tune spread: The Beam Ionization Profile Monitors (BIPM) installed in LEIR allow to measure the transverse beam sizes along the cycle. The normalized emittances can be reconstructed using the optics functions of the MADX model and the rms momentum spread measured with the longitudinal Schottky monitor (typically around 0.1% after cooling). Figure 4.4 shows the normalized transverse emittances, the intensity along the cycle, and the calculated maximum transverse direct space charge tune shift relative to the bare working point.

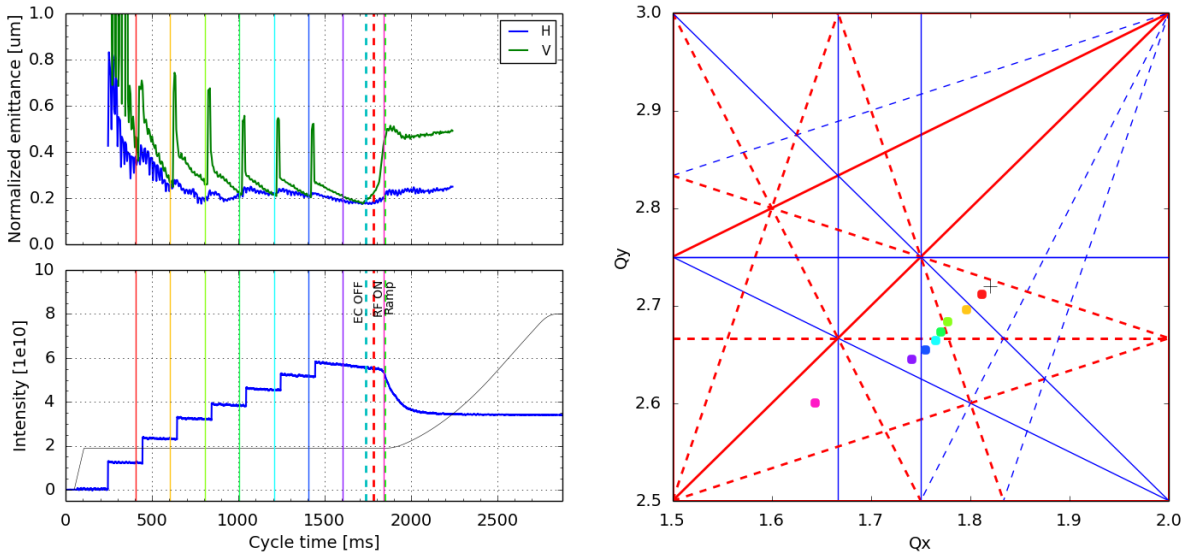

Figure 4.4 Normalized transverse emittances and intensity along the LEIR cycle (left). For the cycle times marked by the coloured vertical lines, the markers with the same colour code indicate the corresponding maximum space charge tune shift relative to the bare working point, which is marked by a cross (right). Solid lines in the tune diagram correspond to normal resonances, dashed lines to skew resonances.

The space charge tune shift increases along with the injections as more and more intensity is accumulated and the transverse emittances reach similar values after cooling. The vertical emittance starts increasing as soon as the electron cooler is switched off, and even more strongly during the RF capture. Enhanced losses are observed when the beam is bunched, which is exactly the moment of largest tune spread due to transverse space charge. In particular, the tune spread covers several betatron resonances (skew and normal) of third and fourth order. The tune spread decreases when the beam is accelerated due to the $1/\beta\gamma^2$ dependence of the space charge force.

Losses during tune scan with low intensity beam: Dynamic variation of the tunes along the injection plateau showed significant losses in the vicinity of low order resonances. In order to minimize the tune spread due to space charge, these tune scans were performed with low beam intensity (only one injection from Linac3). Figure 4.5 shows an example, where the vertical tune was moved from the nominal working point with Qy = 2.72 downwards by about 0.05 within a few hundred ms. Only small losses are observed close to the fourth order 2Qx + 2Qy = 9 resonance. However, significant losses are observed when the vertical tune approaches the skew third order resonance 3Qy = 8. Similar measurements where performed to probe other low order resonances. Significant losses could also be observed close to the Qx + 2 Qy = 7 normal sextupole resonance.

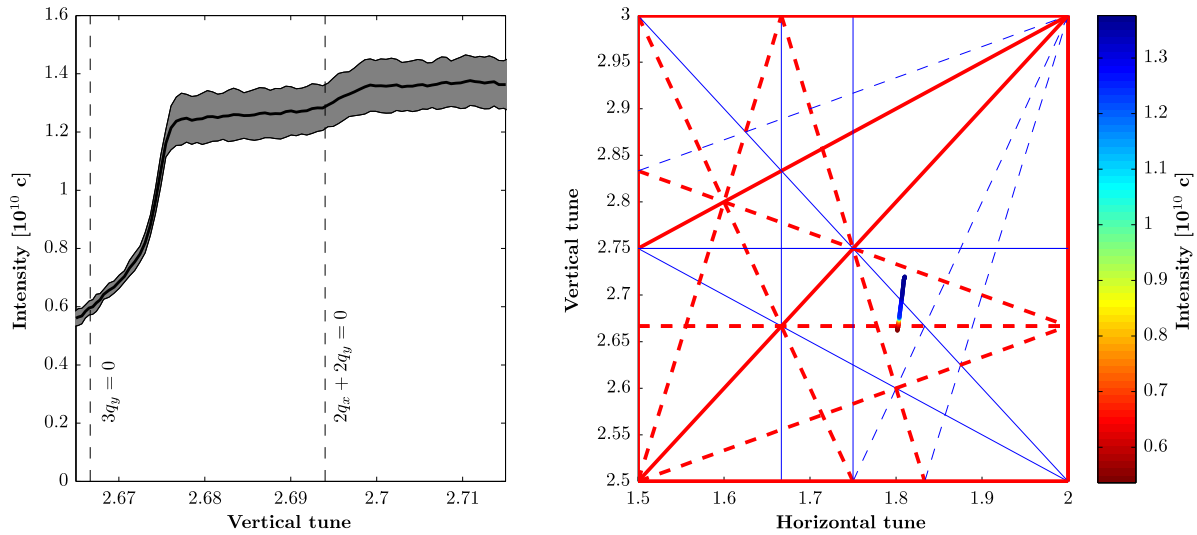

Figure 4.5 Losses during a tune scan with a low intensity coasting beam. Intensity evolution plotted as function of the vertical tune (left) and plotted in the tune diagram (right). Solid lines in the tune diagram correspond to normal resonances, dashed lines to skew resonances.

Effect of harmonic sextupoles on losses: Two independently powered normal sextupole correctors and two independently powered skew sextupole correctors are installed in the dispersion free straight section accommodating the LEIR extraction septum. Following the observations of strong losses close to sextupolar resonances with low beam intensity, a first attempt was made to use these harmonic sextupole correctors to compensate resonances. It was not possible to measure resonance driving terms in 2015 and therefore an empirical approach was chosen: the sextupole current was systematically scanned to optimize the transmission throughout the cycle. An optimal setting with less than 2 A in all the correctors (compared to the maximum of 10 A) could be identified. Figure 4.6 shows the evolution of the accumulated intensity and the intensity at the end of the cycle as function of time. Compared to standard operation without harmonic sextupole correctors, about 10% higher intensity could be accumulated and extracted out of LEIR with the values found in the scans.

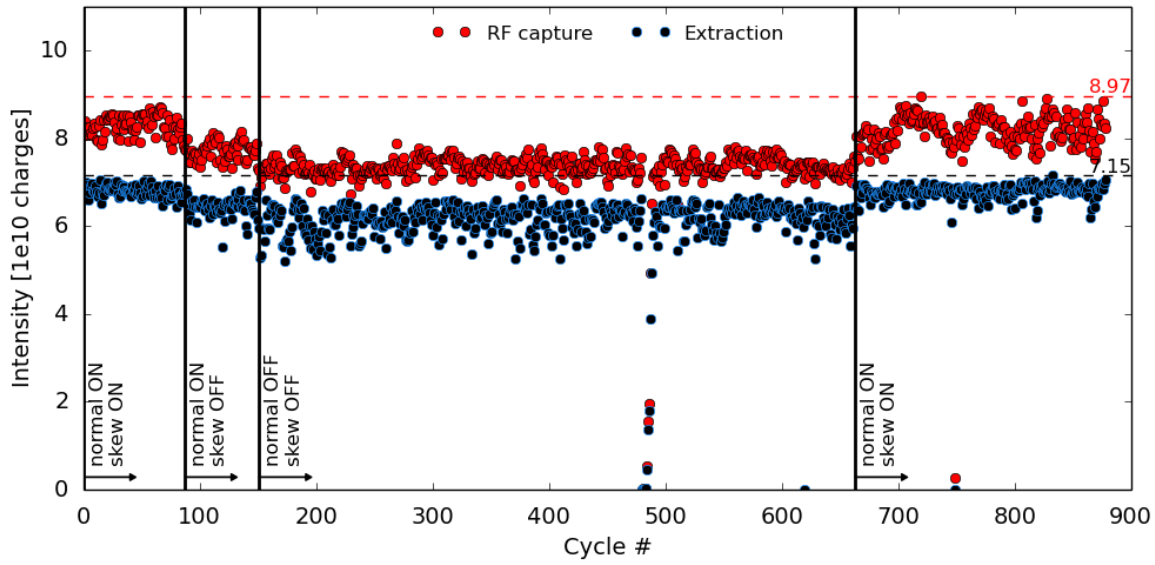

Figure 4.6 LEIR intensity with and without harmonic sextupoles powered. The red and black dashed lines indicate the maximum achieved intensity at RF capture and extraction, respectively.

4.3 LEIR performance in 2015

The operational performance of the lead ion beams for the LHC profited from the efforts during the LEIR machine development sessions described above. Figure 4.7 shows the evolution of the total intensity after accumulation in LEIR, the intensity extracted out of LEIR and, for comparison, also the intensity of the first injection from Linac3 throughout December 2015. The intensity in LEIR is strongly correlated with the current provided by Linac3. However, it should also be stressed that the first attempt of resonance compensation using the existing harmonic sextupole correctors of LEIR yielded a clear improvement of the transmission in the last week of the run.

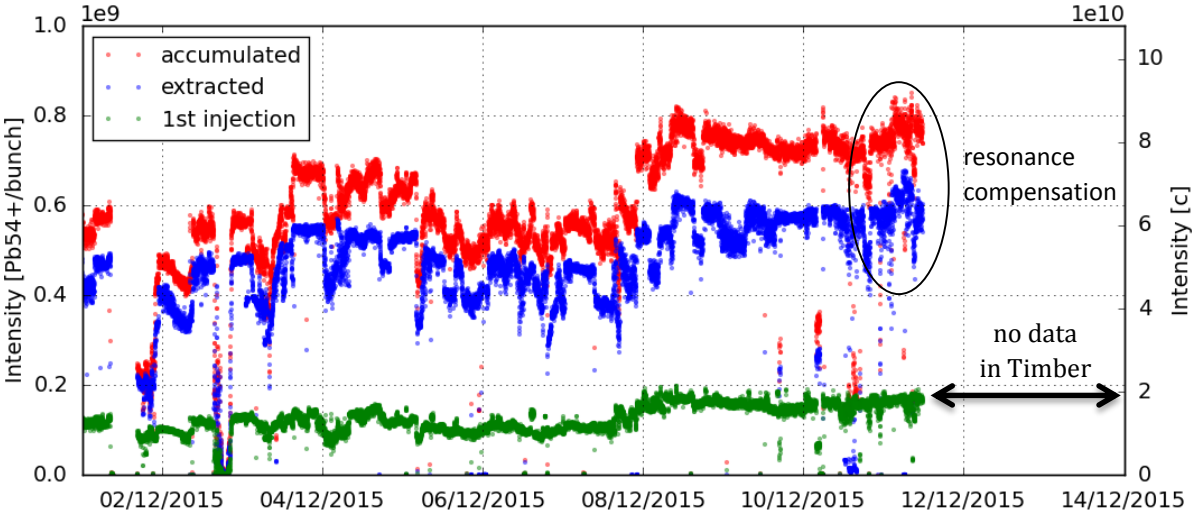

Figure 4.7 Intensity evolution for the "Nominal" LEIR cycle used for LHC filling in December 2015.

Figure 4.8 shows the intensity extracted out of LEIR as function of the accumulated intensity for the same data as shown in Figure 4.7, i.e., of the "Nominal" cycle during the last two weeks of the 2015 lead ion run. The transmission started to degrade slightly for accumulated intensities above 5.0×10^8 ions. However, good transmission could be achieved also for high intensity once the harmonic sextupoles were switched on (see Section 4.2). It appears that extracting higher intensities out of LEIR should be possible in the future, in case the number of accumulated ions can be increased.

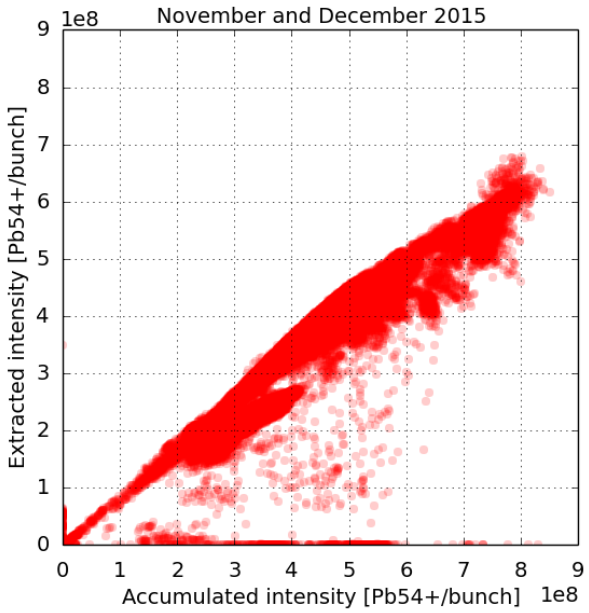

Figure 4.8 Correlation between accumulated and extracted intensity.

4.4 Strategy for reaching the LIU target intensity

In the LIU era, LEIR is requested to deliver two bunches containing 7.4×10^8 ions, which is 25% above the stable operating intensity of 6.0×10^8 achieved in the last Pb^{54+} ion run in 2015. Based on the understanding that the intensity limitation in LEIR is caused by the direct space charge tune spread after the beam is bunched, further improvement in the intensity out of LEIR relies on the following improvements and optimizations:

Increased number of injections by reducing the spacing between Linac3 pulses to 100 ms: In the LIU era, the injection rate will be doubled from 5 Hz to 10 Hz (see Chapter 3). First experimental studies with the increased injection rate will be possible (with a limited duty cycle) in 2016. In order to achieve sufficient cooling of the beam in between injections, it is planned to double the electron current of the electron cooler from 200 mA to 400 mA, which is possible using the existing hardware. It is expected that the accumulated intensity can be increased significantly, since a total of 13 Linac3 pulses instead of the 7 presently used can be accommodated on the injection plateau of the 3.6 s LEIR cycle.

Reduction of the direct space charge tune spread through longer bunches: Optimization of the longitudinal emittance before RF capture and of the capture process itself should allow to slightly increase the bunch length and the longitudinal emittance of the bunched beam. Exploring the limits of this approach will require operating both RF cavities at the same time, which is presently not possible with the existing low level RF system. This feature is a requirement for the new low level RF system, presently under development (see Section 4.5).

Optimization of the resonance compensation scheme, or a working point further from critical resonances: Based on the promising results of the machine development sessions in 2015, further effort will be put in optimizing the resonance compensation scheme. Turn-by-turn position acquisitions will

become available in 2016, enabling the measurements of resonance driving terms and the optimization of the harmonic sextupole strengths. An interesting option is also to change the optics of the machine in order to operate at a working point further away from low order betatron resonances. Due to the stringent constraints on the optics function at the injection point and in the electron cooler [1], finding a suitable optics will require detailed studies.

Further studies and machine development will be critical in the 2016 running period in order to quantify and refine these measures.

4.5 RF System

Capture and acceleration of the ions is performed with a wide-band coaxial Finemet-based cavity and a tetrode based amplifier [2], designed to work in a frequency range of 0.36 – 5 MHz, covering h=1 and h=2 (potentially also h=3) acceleration to top energy (with some margin for lighter ion types). In total two of these cavities, amplifiers and power supplies are installed, one being considered as a hot spare for operation.

The low level RF control is made with a digital system [3], based on custom-made boards including Analog Devices DSPs and Stratix FPGAs. This system has been the first digital control system deployed for circular accelerators at CERN and implements the frequency program as well as beam-related loops (phase, radial and synchronisation at extraction) and the voltage and phase loop on two harmonics for one Finemet cavity. It relies on an obsolete VME front-end processor and will be renovated to the latest generation of digital low level RF (DLLRF), successfully deployed in 2014 on the four PS Booster rings.

The increased processing power available in the new DLLRF will allow further improvements. For instance, both installed cavities could be operated simultaneously for machine development, in order to increase the total RF voltage available and increase the RF bucket area, both for single (h=1) and double (h=2+4) harmonic capture and acceleration, thereby reducing the space-charge tune shift. If this scheme is successful, it will require a review of the risks associated with using both cavities (along with their amplifiers and power supplies) for operation.

4.6 LEIR external beam dump

4.6.1 Introduction

At the moment all beams which are accelerated in LEIR but not requested by the LHC, are either lost on the PS injection septum, or worse, inside the LEIR machine itself. This situation is deemed intolerable for the higher intensity of the LIU IONS beam, which should be disposed of cleanly and safely. A new beam dump is being designed to this effect between LEIR and the PS.

4.6.2 Principle

The new dump will be installed in the “PS switchyard”, at the exit of magnet ETL.BHN10, close to the end of the bi-directional LEIR transfer line ETL (see Figure 4.9).

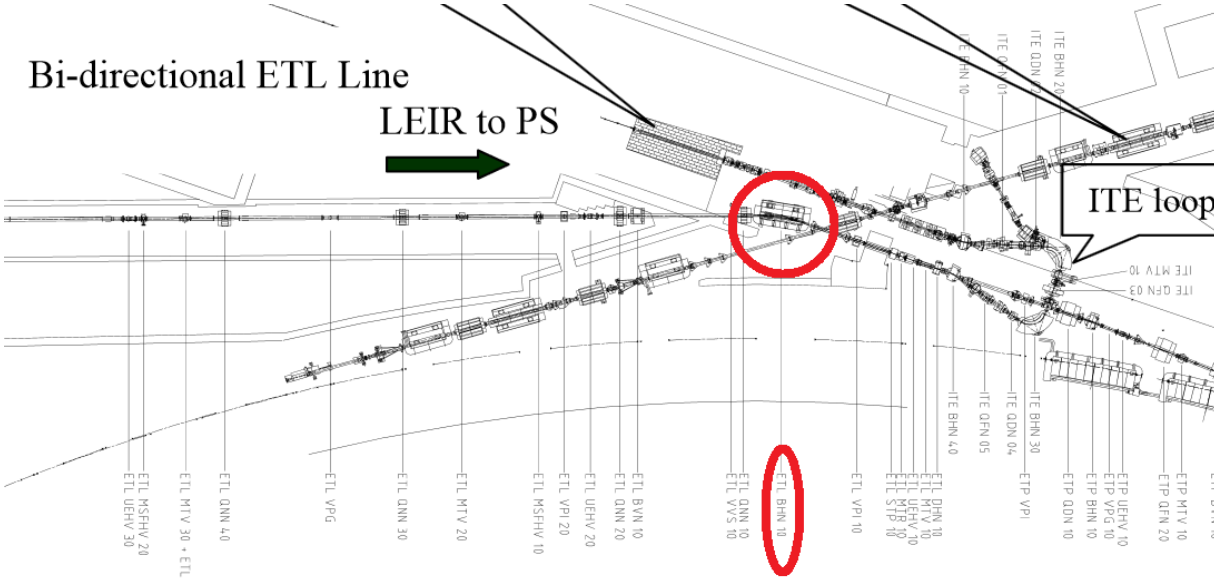

Figure 4.9 Location of ETL.BHN10.

ETL.BHN10 is operated by a function generator, which dispatches for each user the two different values respectively for injection and extraction. At extraction, it normally bends the beam trajectory by 336.75 mrad towards the PS. In order to send the beam to the dump, the magnet will have to be powered by a smaller current. However, for hysteresis reasons, the nominal current will always be sent first (see Figure 4.11) [4]. The vacuum chamber inside ETL.BHN10 will be replaced by a "Y" chamber with the dump at its end. The exact geometry is still being finalized.

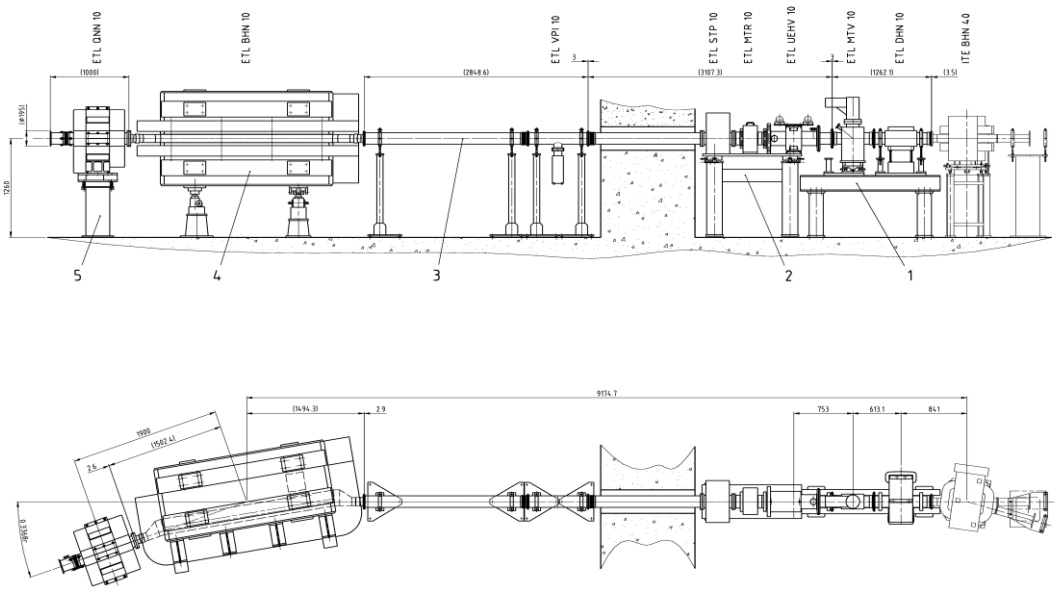

Figure 4.10 ETL.BHN10 implementation (from PS_LMETL0002).

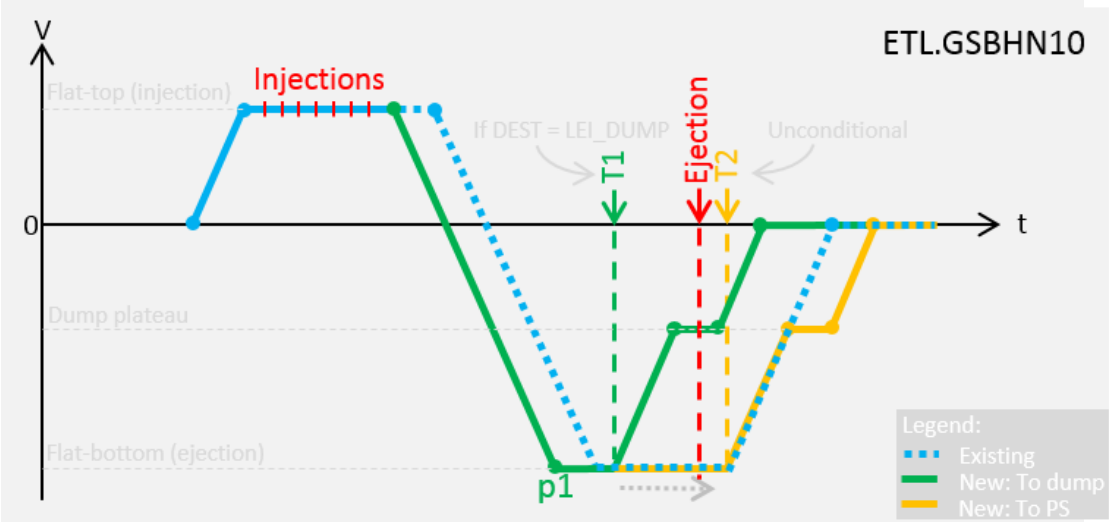

Figure 4.11 ETL.GSBHN10 function adapted for LEIR dump.

4.6.3 Operational details

At first approximation, the new dump has to be designed for continuous beam operation 24h/day, 7 days a week. Heavy ion operation for the LHC is supposed to last until 2029, hence the dump lifetime should exceed the three years duration of a standard LHC Run, so it would only have to be replaced during one of the long shutdowns. It should ideally be installed during the 2017/18 YETS, after the end of the Xenon operation. Relevant beam parameters are listed in Table 4.1.

Table 4.1 Beam parameters relevant for the design of the beam dump.

Ion species	Pb 54+
Energy	72 MeV/u
Intensity	Up to 4e9 ions / cycle
Maximum repetition rate	1 cycle / 2.4 second
Horizontal beta function	30 m
Vertical beta function	10 m
Pulse length	700 ns
Beam structure	2 bunches of 200 ns (spacing 300 ns)
RMS beam width	6 mm
RMS beam height	4 mm

4.6.4 Conceptual design

The proposed design consists of an aluminium block as beam absorber material as shown in Figure 4.12. Since this block must be installed inside vacuum (to avoid the use of windows, which would absorb significant energy in this specific case), the foreseen solution integrates the absorber block and a section of a vacuum chamber. This part could either be machined out of a single aluminium block or, if robust and reliable enough, the dump core could be welded to an aluminium pipe. Aluminium fins are proposed as part of the design in order to cool the dump by natural convection with the air in the area. A stainless steel flange will be integrated to the vacuum chamber in order to reach the required performance in

terms of vacuum tightness. This type of flange has already been successfully used at CERN (e.g. drawings PS_IVC__0026, 27, 28 and 46).

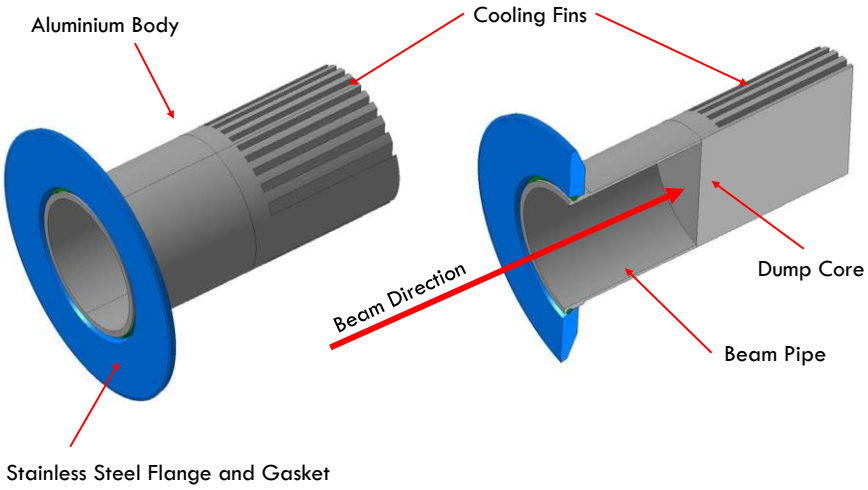

Figure 4.12 LEIR Dump – Conceptual design.

4.6.5 Schedule and Costs

The time required from the beginning of the studies (detailed FLUKA and thermo-mechanical calculations) up to the installation of the device, was estimated to be about two years. The baseline is therefore to have the dump designed (with integration study) by autumn 2016, and subsequently manufactured to be ready for installation during the YETS 2017-18. The present cost estimates do not include any cost related to shielding (if necessary), while the additional costs for modifying the vacuum chambers inside the ETL.BHN10 magnet are included within the vacuum work package.

4.7 Beam Instrumentation

Beam instrumentation is critical for commissioning and understanding accelerators, and LEIR has a limited set of instrumentation in both the injection/extraction transfer lines and the ring.

In order to be able to improve the steering of the beam in the transfer line from Linac3 to LEIR (ITE-ETL-EI), as well as the matching at injection into LEIR, a set of nine new double-plane beam position monitors will be installed during the EYETS 2016-17. These new monitors will be very useful to study systematically the effects of the stray field from the PS onto the transfer line trajectories and generate a steering correction algorithm for this stray field, which is expected to significantly improve reproducibility.

Additionally, the acquisition electronics of the ring orbit measurement system will be upgraded (using the synergy with the ELENA design) to enable turn-by-turn and bunch-by-bunch acquisition of the beam positions. This will allow measuring the optics functions and deriving the resonance driving terms, which can be used for characterising and correcting the machine nonlinearities. However, the upgrade of the electronics only constitutes the first stage of the full consolidation of the LEIR orbit system, because cables and front-end amplifiers will be replaced only after LS2.

4.8 References

[1] LHC Design Report, Volume III The LHC Injector Chain, Editors: M. Benedikt, P. Collier, V. Mertens, J. Poole, K. Schindl, CERN 2004-003, (2004).

[2] R. Garoby et al, *The LEIR RF system*, WPAT018 in Proc. 2005 Particle Accelerator Conference, Knoxville, Tennessee, (2005).

[3] M.E. Angoletta et al, *Beam Tests of a New Digital Beam Control System for the CERN LEIR Accelerator*, WPAT019 in Proc. 2005 Particle Accelerator Conference, Knoxville, Tennessee, (2005).

[4] S. Jensen, *Control system changes required to integrate LEIR dump*, EDMS 1604688.

5 PS

The LIU baseline does presently not foresee any dedicated hardware upgrade, but is only based on an updated production scheme for the nominal beam with bunch splitting.

5.1 RF manipulations in the PS for lead ions

RF manipulations in the PS must adapt one or two almost 200 ns long bunches received from LEIR to the 5 ns long buckets in the SPS. Depending on the scheme, each of the bunches may also be split in the PS. The flexibility of the PS RF systems allows to generate different batch lengths, as well as bunch spacings at extraction. With the so-called nominal scheme [1], four bunches spaced by 100 ns are produced. Intermediate schemes with two bunches at PS extraction result in 100 ns or 200 ns bunch spacing. In the pre-LS1 era the collisions in the LHC only took place with the latter intermediate scheme, with two bunches spaced by 200 ns transferred to the SPS [2]-[4]. The nominal scheme with four bunches has actually not yet been taken by the LHC for luminosity production. Compared to the two-bunch schemes, the intensity per bunch is a factor of two lower for the nominal scheme due to the bunch splitting at intermediate energy in the PS, but twice more bunches are delivered per PS extraction. The basic RF manipulation schemes available for lead ion beams are summarized in Table 5.1. The two main schemes relevant for the LIU upgrades are the single bunch beam for commissioning and 4 bunches spaced by 100 ns. Potential alternative schemes are discussed in Chapter 7.

With the higher intensity out of LEIR aimed at by the LIU project, the original four-bunch scheme will again become the preferred baseline production scheme.

5.2 The nominal four-bunch scheme

The nominal four-bunch scheme had originally been foreseen for the lead ion operation periods during the first run of the LHC [1]. Batches of four bunches spaced by 100 ns are produced in the PS.

Table 5.1 RF manipulation schemes for lead ion LHC-type beams in the PS.

	Single bunch (early)	**4 bunches, 100 ns** (nominal)	2 bunches, 200 ns (intermediate)	2 bunches, 100 ns (intermediate)
Injection				
Number of bunches	1	2	2	2
Intermediate flat-top				
RF manipulations on		Batch expansion, splitting	Batch expansion, re-bucketing	Batch compression
Harmonic sequence	16	16 → 14 → 12 → 24 → 21	16 → 14 → 12 → 24 → 21	16 → 18 → 21
Acceleration and flat-top				
RF harmonic RF manipulation	16	21 Re-bucketing to h = 16/21 → 169	21	21
Ejection				
Number of bunches Bunch spacing	1	4 100 ns	2 200 ns	2 100 ns

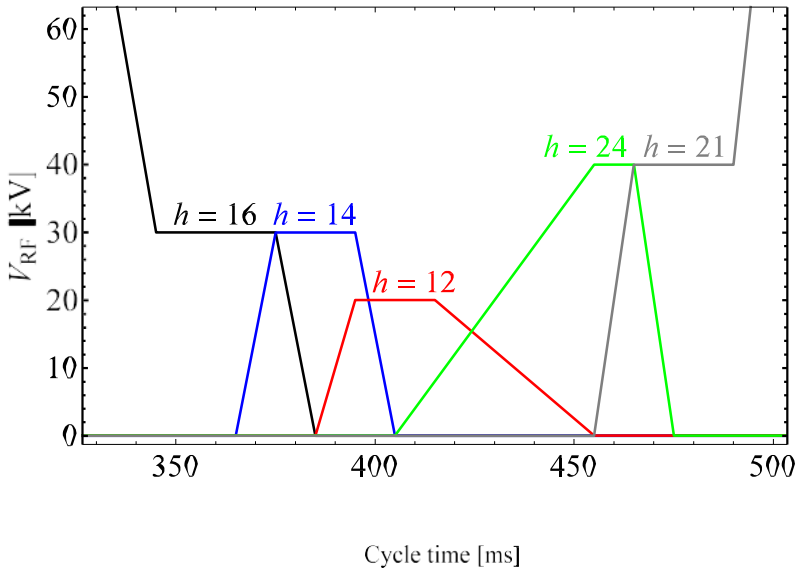

Figure 5.1 Voltage program during the RF manipulation on the intermediate flat-top for the generation of four bunches spaced 100 ns.

Table 5.2 Parameters of the single-bunch and nominal lead ion beams at PS extraction after the upgrades [5].

		Single bunch	4 bunches, 100 ns
Number of bunches		1	4
Longitudinal emittance per bunch	[eVs]	10.4	10.4
Bunch length	[ns]	<4	<4
Bunch spacing	[ns]		100
Intensity	[10^{10} ppb]	1	1

The commissioning of this production scheme had been completed in 2009, but finally the LHC was operated for luminosity production during its first run using a slightly modified scheme, with the splitting replaced by a re-bucketing. It yields only two bunches with double intensity spaced by 200 ns delivered by the PS (Table 5.1, third column).

The voltage programs for the different harmonics during the RF manipulation for the nominal four-bunch scheme are illustrated in Figure 5.1. Two bunches are injected into adjacent buckets at harmonic h = 16 in the PS, the circumference of LEIR being 1/8th of the circumference of the PS. The bunches are first accelerated on h = 16 to an intermediate flat-top at a kinetic energy of approximately, E_{kin} = 0.38 GeV/u.

The distance between bunches is then enlarged from 186 ns to 248 ns by a two-step batch expansion, reducing the main RF harmonic from h = 16 via 14 to 12. The batch expansion is followed by a bunch splitting from h = 12 to h = 24 yielding four bunches spaced by 124 ns. Figure 5.2 shows the measured evolution of the bunch profile during the RF manipulation at the intermediate flat-top according to the voltage programs of Figure 5.1. A final batch expansion step then hands the batch of four bunches over to harmonic h = 21 for acceleration to the flat-top. The bunch spacing shrinks during acceleration to a final value close to 100 ns.

To finally fit the bunches into the 5 ns long buckets in the SPS, a re-bucketing from h = 21 to 300 kV at h = 169 is applied by operating an 80 MHz cavity at a frequency of 79.9 MHz, hence 230 kHz below its frequency of operation for protons. Thanks to the proximity of the extraction energy (γ = 7.3) to transition (γ_{tr} = 6.1) and the well preserved longitudinal emittance, operational experience with the lead

ion beam has shown that no bunch rotation is needed before the transfer to the SPS. The matched conditions at full voltage from one 80 MHz cavity is sufficient to keep the bunch length below 4 ns with the present longitudinal emittance of about 10 eVs.

The longitudinal parameters of the lead ion beam at PS extraction are summarized in Table 5.2. Single and multi-bunch beams have the same longitudinal characteristics and intensity.

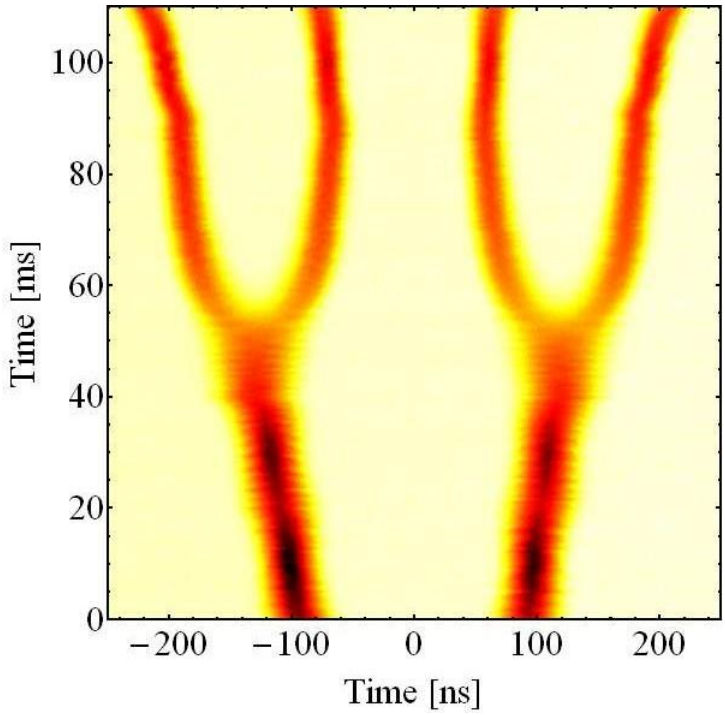

Figure 5.2 Evolution of the bunch profile during the RF manipulation at the intermediate flat-top for the nominal four-bunch beam with 100 ns spacing.

5.3 Other production schemes

Suppressing the bunch splitting and shortening the harmonic number sequence, two bunches spaced by either 100 ns or 200 ns can be generated. In the first case, the bunches are kept in adjacent buckets and handed over from the initial RF harmonic, h = 16, to 18 and then to 21. To generate a bunch spacing of 200 ns, the harmonic number sequence becomes h = 16, 12 and 21. Hence the bunch spacing is first enlarged when moving to h = 12, which is then followed by a re-bucketing to h = 21 leaving an empty bucket between both bunches. The beam delivering two bunches at a spacing of 100 ns (see Table 5.1, right column) has been commissioned in 2014 and was used in the LHC for luminosity production during the 2015 lead ion run.

Alternative schemes to possibly achieve a bunch spacing of 50 ns or shorter, or longer batches, have been studied for possible application in the PS and are addressed in Chapter 7.

5.4 References

[1] LHC Design Report, Volume III The LHC Injector Chain, Editors: M. Benedikt, P. Collier, V. Mertens, J. Poole, K. Schindl, CERN 2004-003, p. 166 (2004).

[2] D. Manglunki et al, *Ions for LHC: Performance of the Injector Chain*, IPAC11, San Sebastián, Spain, 2011, p. 2529.

[3] D. Manglunki et al, *Performance of the CERN Heavy Ion Production Complex*, IPAC12, New Orleans, Louisiana, USA, 2012, p. 3752.

[4] D. Manglunki et al, *The First LHC p-Pb Run: Performance of the Heavy Ion Production Complex*, IPAC13, Shanghai, China, 2013, p. 2648.

[5] H. Damerau, S. Hancock, M. Schokker, *Longitudinal Aspects of Nominal Pb*54+ *Ion Commissioning in the PS*, unpublished presentation at Machine Studies Working Group, CERN, Geneva, Switzerland, 2009.

6 SPS

The baseline for the SPS is to accumulate trains of 4 bunches at 100 ns, with a 150 ns spacing between injected trains. Multiple injections for the PS to the SPS are needed to maximize the number of bunches in the SPS for a given bunch spacing. The optimum number of injections depends on many factors including the lifetime, transmission and blowup in both the SPS and LHC [1]. Slip-stacking will be used to create trains of 8 bunches with 50 ns bunch spacing and 100 ns between trains. By means of a model based on the fit of intensity decay data measured in 2015 in both SPS and LHC, it was found that 12 injections from the PS into the SPS lead to the maximum number of ions at the end of the LHC injection process [2]. This would give 48 bunches in a train of 2.6 μs length after the slip stacking. The duration of the SPS injection flat bottom is then (12 – 1) × 3.6 s, i.e. the first injected bunch has to wait 39.6 seconds before being accelerated.

The upgrades needed are to the MKP injection system for 150 ns rise time (already deployed), the RF Low Level for slip-stacking, and the transverse damper for compatibility with the ion acceleration and the slip stacking. In addition, beam loss and emittance growth in the SPS can also be further investigated and possibly reduced. The beam dynamics aspects and planned system upgrades are described in the following sections.

6.1 Beam dynamics and measurement results

In 2015 a series of measurements were made to characterise the performance of the ion beam with high intensity with the Q20 optics. The beam transmission was comparable to that obtained during past runs with the Q26 optics. The transmission from injection to 450 GeV proton equivalent is observed to depend strongly on the injected intensity, as can be seen in Figure 6.1, with indications of a ‘knee’ in the curve at around 3×10^8 ions per bunch injected. Values obtained are about 60% at injected bunch population of 2.5×10^8 ions/bunch, decreasing to 45% for 5×10^8 ions/bunch. As discussed in Section 2.2, the assumed value for the LIU ions baseline is 2.6×10^8 ions/bunch injected, which can be assumed to lead to 1.7×10^8 ions/bunch extracted with an optimistic transmission of 65%. From Figure 6.2, the main effect is seen to come from the injection plateau, or Flat Bottom, as the transmission through the ramp is essentially independent of intensity, at around 75%. Concerning the transverse emittance growth, its value averaged over a full train injected into LHC was found to be around 40-50% for rms bunch intensities of 2.2×10^8 ions/bunch at SPS extraction. This could be estimated comparing the emittance measurements in the SPS injection line and those at the LHC injection. This high value depends on both the large bunch intensities and the length of time each bunch has stayed at injection energy in the SPS. A target value of 30% is taken for the SPS budget in the LIU beam parameter table.

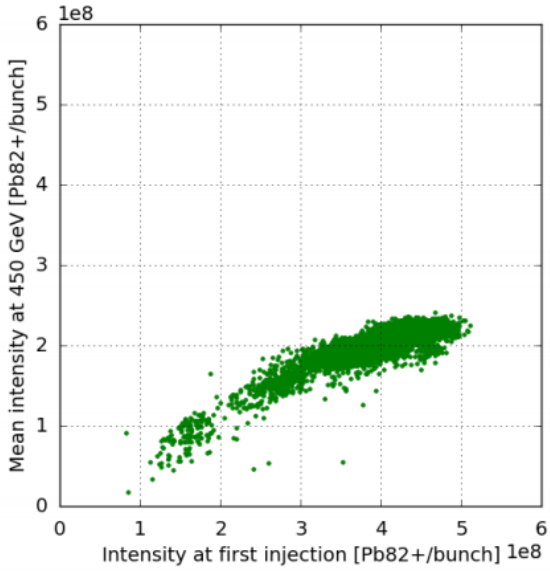

Figure 6.1 Intensity at 450 GeV proton equivalent as a function of injected bunch population, showing a strongly non-linear dependence on intensity.

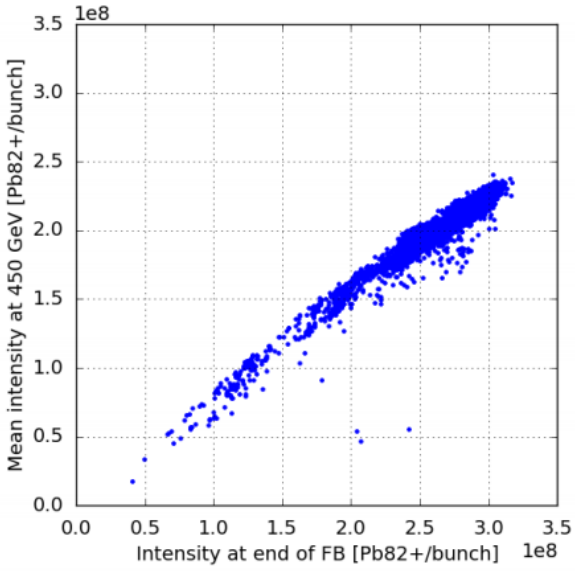

Figure 6.2 Intensity at 450 GeV proton equivalent as a function of bunch population at the beginning of the accelerating ramp, showing a rather linear dependence on intensity.

Overall the SPS degrades the brightness of the ion bunches by a factor 2, most of which comes from losses. With such large loss levels, the SPS transmission is clearly an important target for improvement across the ion chain, in order for the LIU beams to approach the HL-LHC request. The emittance is less significant in terms of integrated HL-LHC performance, in the strongly levelled regime – nonetheless this is also important to understand and control, as the loss mechanism is also very likely related to the emittance growth.

To date the mechanism causing these losses and emittance blow-up could not be clearly identified, with some preliminary studies showing that Intra Beam Scattering (IBS) is not sufficient to explain the observed beam lifetime [3]. A more refined model seems to point to losses created by interplay between direct space charge, Touchek effect and IBS. Systematic measurements were performed in 2015 with

scans of the working point while recording losses, bunch length and emittance on flat bottom, and measurements of emittance evolution along the Flat Bottom for nominal working point. Further measurements are planned for 2016, with characterisation of the loss dependence on intensity and, if possible, an optimization of the working point in order to minimize beam losses and emittance blow-up. In addition, a comparison of losses between FFA (Fixed Frequency Acceleration) and FHA (Fixed Harmonic Acceleration) will be made for operational intensity. Measurements have been made in the past with low intensity and their results are very promising. Finally, if time allows, a comparison of Q20 and Q26 optics, in particular regarding losses, is needed.

The observations from 2015 also showed that the beam is unstable in the longitudinal plane after transition crossing, see Figure 6.3 (left). A controlled longitudinal emittance blow-up was tried in the PS, Figure 6.3 (right), which improved the situation. Controlled longitudinal emittance blow-up was also tried using the SPS in the single 200 MHz RF system, but could not be made to work. No effect of the batch spacing (150 ns and 175 ns) was seen on the longitudinal bunch parameters.

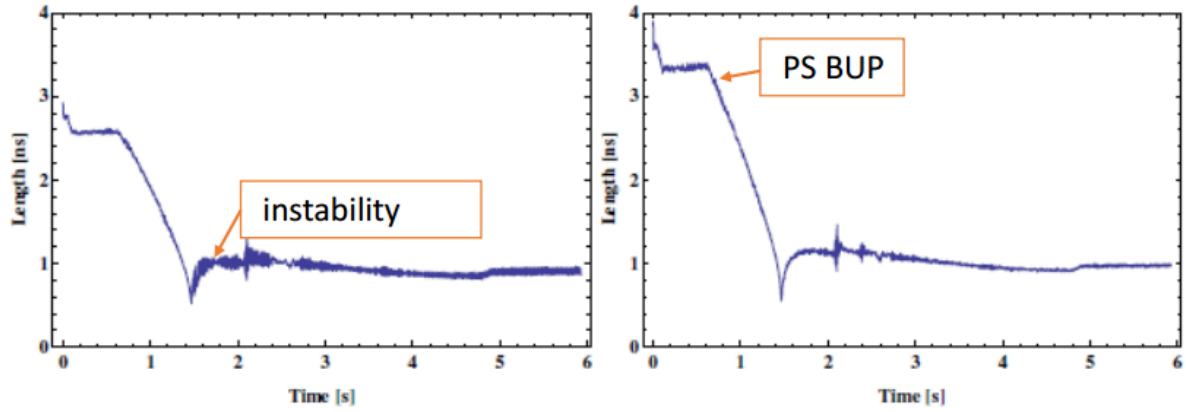

Figure 6.3 Bunch length as a function of time over the SPS cycle, revealing a longitudinal instability after transition crossing (left), which can be improved with controlled emittance blow-up in the PS (right).

Tests were also made in 2015 in preparation for the slip stacking. The momentum aperture was measured at the extraction plateau (Flat Top), with radial steering of the beam. With the extraction bumps switched off (necessary to avoid artificial limits on the extraction septa) the beam could be steered ±20 mm corresponding to a momentum aperture of about ±5×10-3 in Δp/p. The slip stacking has been simulated with ±6 mm (±1.64×10-3 in Δp/p), which means that the available aperture is comfortable.
Additionally, the beam stability was measured with the phase loop switched off, as the phase loop will not work during the several hundreds of ms of the slip-stacking process (see Section 6.2). The beam was observed to survive during 400 ms without the phase loop, without losses, but with a 20% increase in the longitudinal emittance, as evidenced by the observed bunch length increase from 1.3 to 1.45 ns. Together with the expected factor ~3 emittance blowup from slip stacking itself, this may mean that a bunch rotation at extraction or use of the 800 MHz system during slip stacking may be required to meet the target bunch length at transfer to LHC.
In 2015 the transverse dampers were successfully operated with ions. The operation was problematic (as expected) due to the Fixed Frequency Acceleration scheme (Section 6.4.2), which results in the beam position sampling being shifted and bunches essentially assigned to the wrong bucket. Due to the shifting, a correct tagging is not possible and the signal processing "sees" more than 2×12 bunches. The feedback correction signal therefore shifts for subsequent injections. This results in a degraded injection damping for later batches. For most of the ion run the damper was deactivated after the 11th injection, and damping was only active at the Flat Bottom (no feedback during ramp). One of the two horizontal dampers was used, with the feedback phase arbitrarily detuned by +20o, as there were erratic beam losses when using optimum feedback phase. Despite these difficulties the damper worked well for damping the injection oscillations with the 150 ns bunch spacing and increased residual kick (see Section

6.2), with damping times below 1 ms achieved, Figure 6.4. To note that all of these problems will be solved for 2016, when the fibre links ensuring the correct bunch synchronisation will be in place.

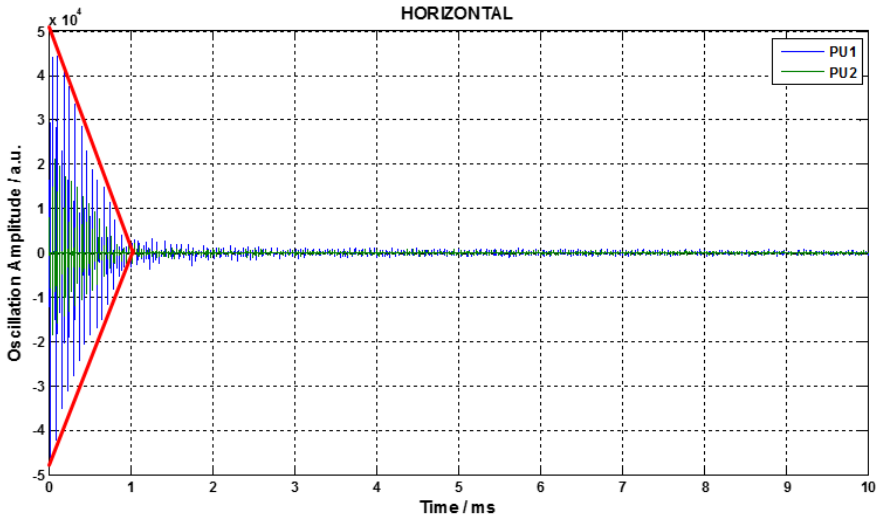

Figure 6.4 Damper performance in 2015 showing damping of horizontal injection oscillations at 150 ns batch spacing within 1 ms.

The beam tail population is expected to increase with 150 ns batch spacing, due to the larger injection offset from the residual kick on both injected and circulating bunches, combined with the finite damping time. To characterise the expected tail population, the detuning with amplitude was measured, by kicking the beam at the Flat Bottom with the tune kickers MKQH/V and using the LHC BPM turn-by-turn data to calculate the action. A linear fit to the data for different amplitudes gives the detuning coefficients, Figure 5, which were measured at c_{xx} = 394.2 m^{-1} and c_{yy} = 1453.1 m^{-1}. This data will be used for simulating the expected tail population.

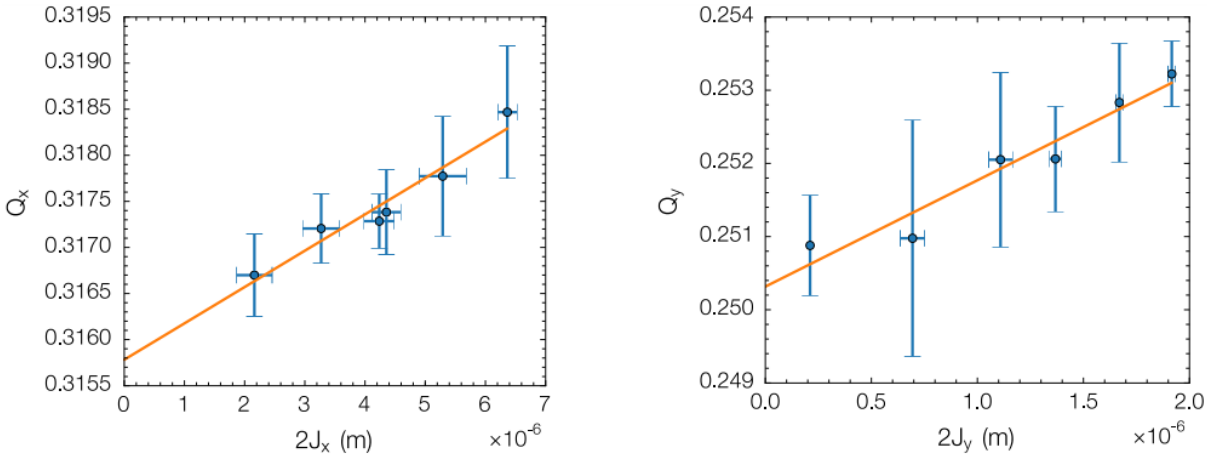

Figure 6.5 Measured horizontal (left) and vertical (right) detuning with amplitude at injection energy. c_{xx} = 394.2 m^{-1} and c_{yy} = 1453.1 m^{-1}.

6.2 SPS injection kicker rise time and bunch spacing at LHC injection

One of the main requirements from the LHC is to maximize the number of colliding bunches. The bunch pattern of six trains of eight 50 ns spaced bunches, separated by 100 ns, per injection into the LHC is realised in the LIU baseline scenario by slip stacking in the SPS (as described in the Section 6.3) of 12 trains of 4 bunches from the PS at 100 ns, with 150 ns spacing between trains. The 150 ns spacing was

deployed in 2015 and is now considered as operational. This was done by reducing the kick angle through the use of an injection bump, which allows operation only with the fastest MKP1-3 generators at the ion injection energy. The synchronisation of the individual thyratrons was also improved with an upgrade of a timing module, and replacement of the worst tubes, gaining over 30 ns in the jitter. As a result, the residual kick for the injected/circulating bunches with 150 ns batch spacing is now less than 5%, as illustrated in Figure 6.6, which was compatible with the performance of the transverse damper and allowed injection without significant emittance growth. To improve further to 100 ns spacing between trains (giving a uniform 50 ns between bunches in the LHC) would require a major redesign of the injection system, the option for which is described in Chapter 7.

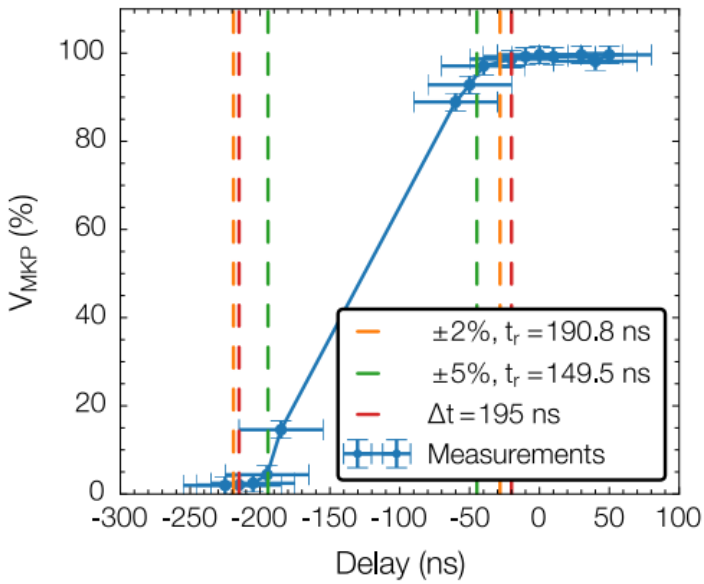

Figure 6.6 Measured MKP rise time after system improvements in 2015, with 150 ns 5-95% achieved.

6.3 SPS slip stacking and LLRF ions upgrade

6.3.1 Introduction

Momentum slip-stacking [4] is planned in the SPS to increase the number of bunches in the LHC-type ion beams by decreasing the bunch spacing from 100/150 ns to 50/100 ns [5]. During this process, which will be made possible after the planned upgrade of the SPS 200 MHz RF systems [6], trains of bunches spaced by 100/150 ns are interleaved producing the desired beam pattern.

Slip-stacking in the SPS with the aim to increase the bunch intensity had been studied earlier for proton [7], [8] and ion beams [9]. A similar procedure can be applied in the case of interposing the two batches. The implementation is favoured by the large bandwidth of the SPS 200 MHz travelling wave RF system (199.5 – 200.4 MHz), which makes possible the performance of the special RF frequency manipulations required. In addition, small initial longitudinal emittances (0.125 eVs/u [10]) and low ion intensities [3] make this solution even more attractive.

The slip-stacking process is shown schematically in Figure 6.7. The batches should be captured independently by two pairs of the 200 MHz Travelling Wave Cavities (TWC). The RF frequencies are then programmed such that the first batch is accelerated and the second is decelerated. Being at different energies, the two batches are slipping towards each other in the azimuthal dimension. After some time, the reverse procedure takes place, where the two batches approaching each other in energy with RF

programs designed accordingly. Once the two bunch trains are close enough in energy and in the correct azimuthal position, they are recaptured at average frequency and filament into a large bucket.

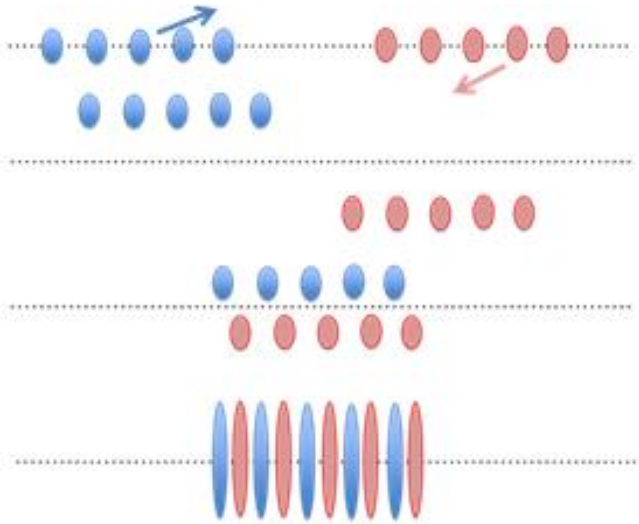

Figure 6.7 Schematic representation of momentum slip-stacking for halving the bunch spacing.

In principle slip-stacking could be applied at flat bottom, at some intermediate energy plateau or at flat top. At flat bottom the effects of IBS, space charge and RF noise, already observed under the operational conditions, make this choice the least favorable. On the other hand, if this RF gymnastics is performed at flat top, any lost beam will be transferred into the LHC. The latter can be significantly reduced if slip-stacking is used at an intermediate plateau with the additional advantage (in comparison with flat top) that no extra time is needed for bunch filamentation, which will take place during the rest of the ramp.

6.3.2 Slip-stacking at 300 GeV/c proton equivalent

For the particle simulations described below (see also [11]), initial conditions at the intermediate flat top (momentum of 300 GeV/c proton equivalent) are presented in Table 6.1.

Table 6.1 Initial conditions used in simulations of slip-stacking.

Parameter	**Symbol**	**Value**	**Units**
Lorentz factor	γ	127	-
Slippage factor	η	$3x10^{-3}$	-
Longitudinal emittance	ε_l	0.125	eVs/u
RF voltage amplitude	V_{RF}	0.34	MV
Small amplitude synchrotron frequency	f_{s0}	68	Hz
Maximum momentum separation per beam	$\Delta p/p$	$1.84x10^{-3}$	-
Maximum radial displacement per beam	ΔR	6.0	mm
Frequency offset per beam	Δf_{RF}	1116	Hz

The SPS optics with lower transition energy (Q20) is assumed and the initial emittance is defined by the maximum value obtained during measurements in 2013, without any controlled blow-up [10]. The initial RF voltage was calculated in such way that the selected bunch size corresponds to a filling factor in momentum of 0.9. The maximum separation in momentum is selected to be significantly larger than the bucket height (but within the aperture limit) in order to reduce the slipping time and minimize the mutual influence of the two beams during this process.

The RF programmes applied for separating the two batches in momentum (RF frequency) and then bringing them back, close to the central orbit, are presented in Figure 6.8. For calculating the RF voltage programme, a constant filling factor in momentum of 0.9 was assumed to avoid particle losses during the procedure. In this case the duration of the slip-stacking process is 200 ms, fast compared to the cycle time (about 50 s), but slow enough to avoid particle losses. However this does not take into account the time of batch slippage after separation, which is determined by initial distance between batches (see below) and possible radial displacement. The final value of the RF frequency was selected such that the ratio $\Delta f_{RF}/f_{s0} = 4$, which corresponds to the case where the final hypothetical buckets have tangent boundaries. In fact, that condition gives a lower limit for stable motion [12], but tracking simulations show that there is a rapid effective emittance growth and that a larger value is needed for stable motion [13].

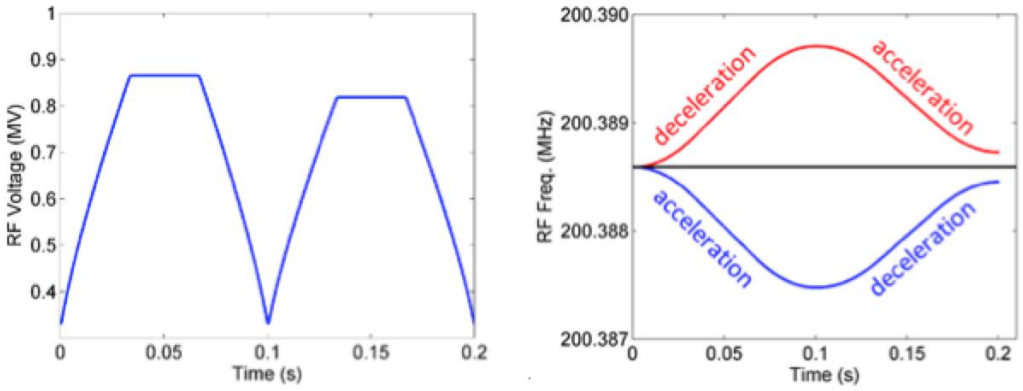

Figure 6.8 RF voltage (left) and frequency (right) programmes used in simulations for slip-stacking.

The capture of bunches by a single bucket of the average RF frequency has to be optimized for minimum losses with a small as possible final emittance. That means that the two batches should be brought as close as possible before recapture takes place. However, as the beams are approaching each other, the interaction due to the two RF systems becomes more dramatic, resulting eventually in particle losses. For the results presented below a high value of the recapture RF voltage was used (3.4 MV) to minimize the losses, at the expense of large emittance dilution (factor of 3). This choice was based on the small initial emittance, which leaves margin for a large blow-up and also on the planned RF power upgrade [6], which will provide the required RF voltage to obtain finally bunch lengths acceptable for extraction into the LHC.

The slippage and recapture parameters as well as the beam characteristics after recapture are presented in Table 6.2. The slipping time of 200 ms is defined by the designed RF programmes. During this time a slipping distance of about 2.4 μs was obtained from the simulations. The latter defines the minimum distance between the last bunches of the two batches, which results in a batch distance T_B of 100 ns since the length of the batch is 2.3 μs. In reality, the minimum distance between the batches is defined by the Low Level RF specifications; it should be large enough to assure that each batch is exposed only to the RF voltage of its corresponding pair of 200 MHz TWC (T_B > 1.3 μs). For example, with a batch

distance of 2.7 μs [10] an extra slipping time of around 100 ms at the maximum momentum separation will be needed. Larger values can be also used at the only expense of increasing the slipping time.

Table 6.2 Slippage, RF and beam parameters after recapture.
The slipping distance corresponds to a batch spacing of 2.7 μs.

Parameter	**Value**	**Units**
Slipping distance	2.5	μs
Slipping time	300	ms
Recapture RF voltage	3.4	MV
Bucket size	0.54	eVs/u
Longitudinal emittance	0.36	eVs/u
Bunch length	3.3	ns

6.3.3 Beam parameters at flat top

After the RF gymnastics is completed and the final beam pattern is obtained, bunches are accelerated to the top energy with a momentum programme calculated again for a constant filling factor in momentum of 0.9. At flat top two possible schemes to provide the final bunch lengths at extraction are considered: a) bunch compression by an adiabatic increase (within 50 ms) of the RF voltage to the maximum available value, similarly to the present situation and b) bunch rotation, by a non-adiabatic RF voltage increase (during 1 revolution turn) to the same value. In addition, two different values of the maximum RF voltage were used, corresponding to the current RF limit ($V_{RF}^{max} = 7.5\ MV$) and the one after the RF power upgrade ($V_{RF}^{max} = 15\ MV$). The results are summarized in Table 6.3, where one can see that a bunch length small enough to be sent to the LHC ($\tau < 1.8\ ns$) can be obtained only in the case of bunch rotation.

Finally, the study was extended to the case of the previous SPS optics with the higher transition energy (Q26), which was replaced by the Q20 optics in 2013. In fact, with the Q20 optics the beam proved to be less sensitive to IBS and a decrease in the space charge detuning was also measured. However, concerning the slip-stacking, the Q26 optics looks more promising due to the larger relative bucket area for the maximum available RF voltage. In this case the final emittance is defined by the RF gymnastics (and not beam stability), while bunch length at extraction (which should be small enough to fit into the 400 MHz LHC RF buckets) is determined by the maximum RF voltage. Thus, Q26 provides a larger margin for the final beam parameters as can be seen in Table 6.3. Note that bunch lengths within the LHC specifications can be obtained even with the present voltage limitations.

Table 6.3 Summary of results of the slip-stacking simulations and beam parameters at extraction.

SPS optics	**Recapture voltage (MV)**	**Final emittance (eVs/u)**	**Losses (%)**	**Bunch length at flat top for different RF gymnastics and voltages**			
				Bunch compressed with 200 MHz voltage		**Bunch rotated with 200 MHz voltage**	
				7.5 MV	**15 MV**	**7.5 MV**	**15 MV**
Q20	3.4	0.35 – 0.36	1 – .2	2.3 ns	1.9 ns	1.8 ns	1.3 ns
Q26	2.0	0.35 – 0.36	1 – 2	2.0 ns	1.7 ns	1.4 ns	1.05 ns

6.4 LLRF ions upgrade

The Low Level RF will be completely upgraded along with the power upgrade of the 200 MHz RF system. This section presents the new LLRF system for the acceleration of LHC ions in the SPS.

6.4.1 Slip stacking and cavity control

To implement slip-stacking two sets of cavities need to be driven with different RF. These RF can be generated locally by offsetting the frequency in the cavity controller of each cavity, or globally by having a DDS (Direct Digital Synthesizer) generating one Master RF per beam. The second option is preferred because such a Master RF is required for the beam-phase loop and to generate beam-synchronous trigger for observation.

During the first part of the slip-stacking process the two batches are adiabatically manipulated at different frequencies. The recapture in a bucket at the common frequency (bucket merging) requires a fast, non-adiabatic, frequency change.

6.4.2 Existing SPS-ions Beam Control

Figure 6.9 shows the present SPS ions-for-LHC Beam Control system. The Master DDS generates a multiple (2^{13} times) of the revolution frequency, via a feedback including phase loop and synchro loop [14]:

- The phase loop minimizes the beam-RF phase noise to avoid longitudinal emittance growth caused by RF noise. It is a fast loop with a reaction time much smaller than the synchrotron period that effectively damps synchrotron oscillations.
- The synchro loop is a slow loop (reaction time larger than the synchrotron period) that controls the average beam energy. It locks the Master RF on a reference frequency that tracks the dipole field (F_{rf} prog on Figure 6.9).

The Master DDS output is used as clock by the Slave DDS that generates two RFs: the Favg (4620 Frev) and the RF_FSK, a signal with a rectangular frequency modulation: a fixed frequency during 2310 periods, and a varying frequency during the rest of the turn so that the total number of periods is 4620. This scheme is called Fixed Frequency Acceleration (FFA) [15]. This architecture has proven to work, except for the high RF noise level which was traced to the Master DDS and which is being improved through an upgrade.

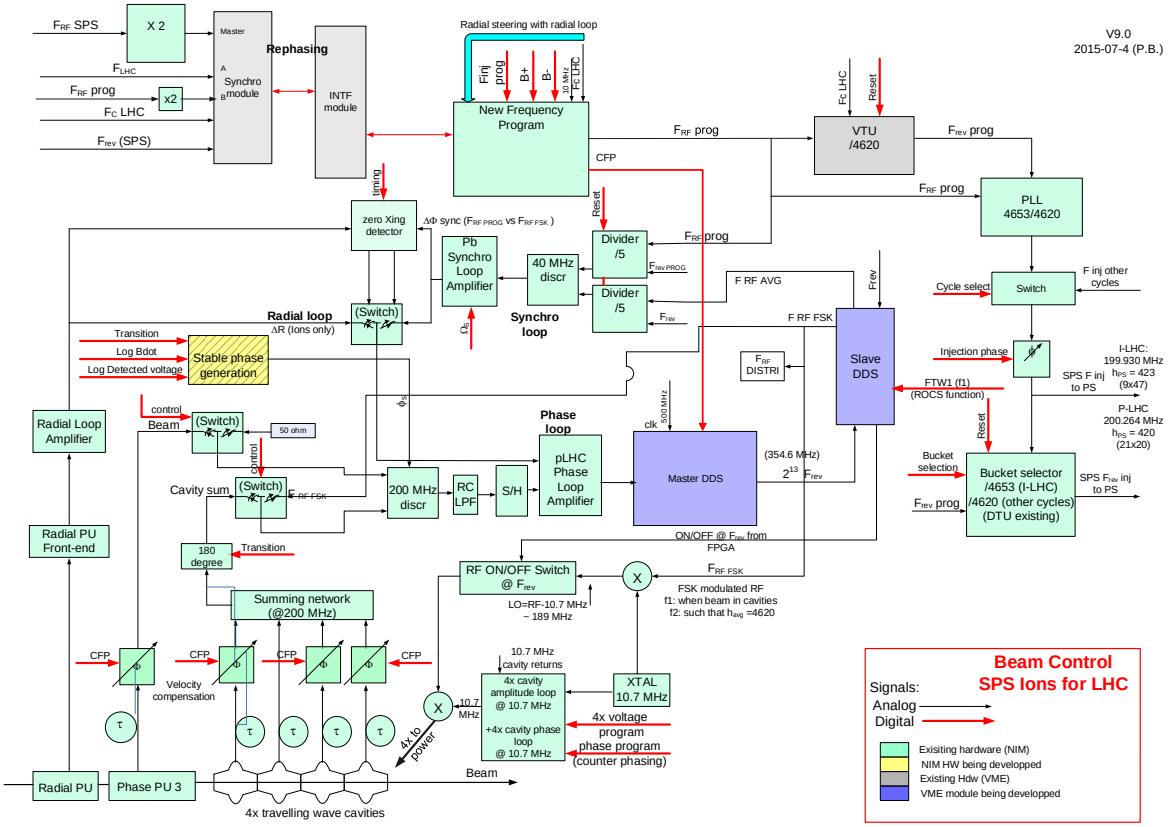

Figure 6.9 Present SPS ions-for-LHC Beam Control for Fixed Frequency Acceleration (FFA).

6.4.3 Proposed new beam control for ions

In the existing system (Figure 6.9), the Master DDS is "fine-adjusted" using Synchro loop and Phase loop signals. The Slave DDS generates one RF sent to "Cavity Controller" RF_FSK, plus Favg=4620 Frev.

This architecture does not require major modifications for slip stacking. We keep one Master DDS only, but now adjust its frequency from the synchro loop only. It does not have a phase loop input. Indeed the Master DDS being common to both beams, it only adjusts its frequency to keep a hypothetic beam centered.

The Slave DDS is upgraded to a Triple Slave DDS. The three RF outputs are:

- Favg= 4620 Frev0. Note that, in slip stacking mode, the Frev0 will refer to neither beam 1 nor beam 2. It is 4620 times the revolution frequency for a beam centered. It will be used as clock for the Cavity Controllers (see below)
- RF_FSK1 that is the master RF beam 1, potentially frequency-modulated (FFA), with an offset (slip stacking) and corrected from the Beam Phase Loop Beam 1 input
- RF_FSK2 that is the master RF beam 2, potentially frequency-modulated (FFA), with an offset (slip stacking) and corrected from the Beam Phase Loop Beam 2 input.

Figure 6.10 shows the modifications proposed to the diagram on Figure 6.9. Generation of the Beam Phase loop signals are discussed later.

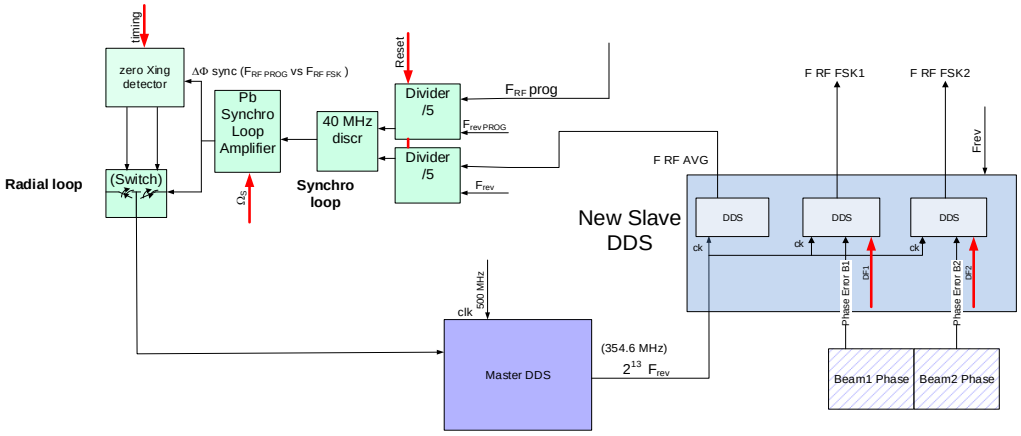

Figure 6.10 Proposed modification to existing system. Master DDS without phase loop correction and New Slave DDS generating two Master RFs, with individual phase loop error signals.

The architecture of Figure 6.10 allows for instantaneous manipulations of the frequency offsets, as desired for bucket "merging".

6.4.4 Cavity Controller

The architecture shown on Figure 6.10 will generate one Master RF per beam. Beside the generation of the Beam Phase measurement, the Beam Control problem seems solved. But the next question is how to make the field in the RF cavities track the Master RF. That is not trivial because:

- The cavity controllers are clocked with Favg=4620 Frev0 (not modulated, centered beam frequency). Modern digital electronics do not appreciate frequency transients in clock signals.
- The Master RF are displaced by frequency offset (slip stacking, +- 1 kHz max) and/or are modulated at Frev (FFA).

In the design of the 800 MHz Cavity Controller, the Sum of the 200 MHz cavities will be used as reference for the 1-T feedback (Figure 6.11) [16]. The situation for ions is similar. We could input the Master RF B1/2 into a Reference channel of the 200 MHz Cavity Controller. This signal will be demodulated using the Favg clock (4620 Frev0). Then, after demodulation:

- FFA and NO slip stacking: the demodulated signal phase is a triangular wave at the exact Frev0. As the 1-T feedback has gain on all multiples of Frev0, it will impose the same field in the cavity.
- NO FFA and slip stacking: then the demodulated signal phase is a linear ramp (modulo +-180 degree), with slope equal to slip stacking frequency offset that is around 1 kHz. The single-sided BW of the 1-T fdbk comb is ~500 Hz. But it can be extended around the first band (DC after demodulation).
- Simultaneous FFA AND slip stacking is excluded [17].

As conclusion, if FFA and slip stacking are not needed simultaneously, it will be fine if we increase the Frev comb filter BW around the first Frev line.

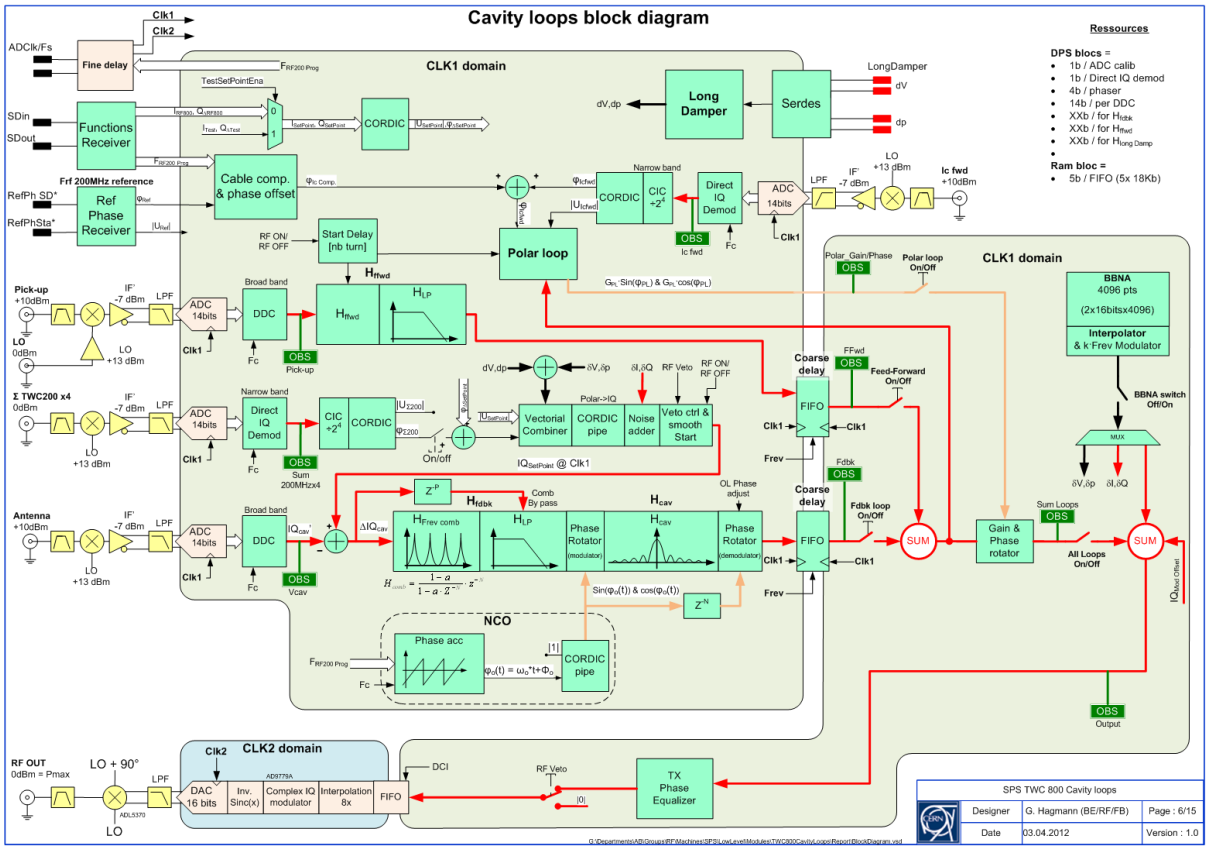

Figure 6.11 800 MHz Cavity Controller.

6.4.5 Beam Phase measurement

The problem is bunch-by-bunch phase measurement in FFA. With FPGA-based electronics, we do not want to clock the digital electronics with a frequency modulated clock (such as F_{rf_fsk}). With ions, bunches are spaced by 50 ns minimum as long as the two batches do not overlap (as during slip stacking). We propose a 2 channels I/Q (or non IQ) demodulator (1 channel = PU signal plus 200 MHz BPF generating a 40 ns long wavelet, second channel = Cavity Sum) with all clocks (and LO) synchronous with Favg. In both FFA and Slip-Stacking the bunch spacing will not be a constant number of clock samples. But this can be dealt with, as long as the single-bunch phase measurement has a flat level extending over more than 1 clock period. We could then use a bunch synchronous signal to identify the exact time-position of the bunch.

At the end of the slip stacking process, when the batches start overlapping, individual bunch phase measurement will not be possible.

6.4.6 Strategy

The design of this Beam Phase measurement system is the most challenging. The second issue is the clocking of the Cavity Controller as explained above. The validity of the proposed solution must be demonstrated.

6.5 SPS Transverse Damper for Ions

The transverse damper system for ions uses the same power system and pick-up hardware as for the proton LHC beams [16]. The operation of the ion beams in the SPS does not need the transverse feedback system for beam stability and the high brightness achieved for ion beams in the SPS up to

2015 was possible without using the transverse feedback system for injection damping. This is different now, with 150 ns MKP rise time, where the injected bunches are subject to more injection kicker ripple and subsequent emittance increase through filamentation.

The upgrade for ions suggested within the framework of the LIU project consists of dedicated electronics to provide the feedback signals for injection damping at fixed kinetic energy of 5.9 GeV/u. The principal difference of the Pb ion scheme with respect to protons at injection consists in the frequency modulation of the RF needed to keep the RF frequency used during the passage of the batch through the cavities with the bandwidth of these. Since the RF cavities and frequency generation are located in BA3 of the SPS and the transverse feedback system in BA2 of the SPS, all signals transmitted from BA3 to BA2 for the transverse damper need to be delayed by a proper amount to keep synchronism between the frequency modulation and the beam signals from pick-ups in BA2. Different delays are required to align the kick signals for the kickers also installed in BA2, but in different locations with respect to the pick-ups. Stabilized optical fibers delay lines will be used for these delays; these are currently under development. The scheme for the delays is outlined in [16].

A separate instance of already developed hardware for the proton LIU damping loop will be used for ions, with FPGA firmware, software, and settings to be adapted for the operation with ions. The operation of the system during acceleration and the slip stacking process is currently not foreseen. However, signals from the feedback system may be used for observational purposes during acceleration and flat top when the beam is bunches, provided clock delays can be appropriately programed during these processes to keep synchronism between sampling, and beam signal. For observation during the slip-stacking process the situation is more difficult as a 200 MHz down conversion cannot be used and one would have to resort to observation in the baseband as also used for the proton transverse feedback for the doublet beam at injection with the added difficulty of having to generate a common sampling signal from the two frequency RF signals used during the slip-stacking. In principle this is not considered impossible but outside the scope of this LIU project.

A study was carried out in 2013 to assess the blow-up at injection from filamentation of injection errors in scenarios with 50 ns and 75 ns batch spacing [18]. Although these short batch spacings are not realistic, the key results of the 75 ns scheme can serve to estimate the performance of the upgraded damper system for larger batch spacing.

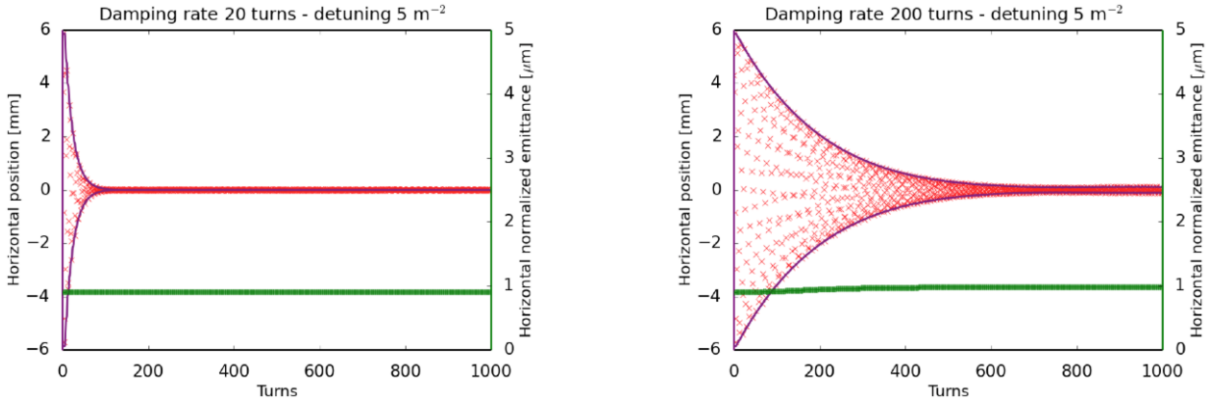

Figure 6.12 Damping of injection oscillation of 6 mm in presence of amplitude detuning with a damping time of 20 turns (left) and 200 turns (right). No blow-up for the 20 turns case and a small blow-up visible for the 200 turns case.

From the 2013 study, a target damping rate of 20 turns was needed to keep the blow-up at injection negligible for the 75 ns batch spacing case with 6 mm injection error (60 m beta, see Figure 6.12). For the scenarios with 150 ns batch spacing the requirements will be similar, i.e. the expected injection error will be comparable and a similar damper time will be required.

6.6 References

[1] M. Schaumann, *Heavy-ion performance of the LHC and future colliders*, CERN-THESIS-2015-195.

[2] H. Bartosik, B. Goddard and G. Rumolo, *LIU beam ion specification*, in LIU Beam Parameter Working Group meeting, 12 February 2016, CERN (2016).

[3] F. Antoniou et al., *Performance of SPS Low Transition Energy Optics for LHC Ion Beams*, TUPME046, IPAC'13, Shanghai, China.

[4] R. Garoby, *RF Gymnastics in a synchrotron*, in Handbook of accelerator physics and engineering, World Scientific ed., 1999, pp 286-287.

[5] D. Manglunki, Performance of the injectors with ions after LS1, in Proc. of RLIUP Workshop, 29-31 October 2013, Archamps, France (2013).

[6] E. Shaposhnikova, E. Ciapala, and E. Montesinos, *Upgrade of the 200 MHz RF System in the CERN SPS*, IPAC'11, San Sebastian, Spain (2011).

[7] D. Boussard and Y. Mizumachi, Production of beams with high line-density by azimuthal combination of bunches in a synchrotron, IEEE Trans. Nucl. Sci. Vol. NS-26 No. 3, 3623, June 1979.

[8] E. Shaposhnikova, T. Argyropoulos, *Possible increase of bunch intensity in the SPS***,** talk at LIU-SPS BD WG, CERN, June 2011.

[9] T. Linnecar, *Azimuthal combination - slip stacking*, Slides, SLI Meeting 2001-10-11, CERN.

[10] T. Bohl, *Slip stacking of the Nominal I-LHC Beam*, Internal Note-2013-26.

[11] T. Argyropoulos, *Momentum slip-stacking of the I-LHC beam in the SPS*, talk at LIU-SPS BD WG, CERN, 27/02/2014.

[12] F. E. Mills, *Stability of Phase Oscillations Under Two Applied Frequencies*, BNL Int. Report AADD176 (1971).

[13] J. A. MacLachlan, *The Beam Dynamics of Slip Stacking*, FERMILAB-FN-0711, Nov. 2001.

[14] P. Baudrenghien, *Beam Control for Protons and Ions*, CERN-OPEN-99-077, 9th LEP-SPS Performance Workshop, Chamonix, France, 25 - 29 Jan 1999.

[15] D. Boussard et al, *Fixed Frequency Acceleration in the SPS*, CERN-SPS/89-49 (ARF).

[16] LHC Injectors Upgrade, Technical Design Report, Vol. 1, Protons, CERN-ACC-2014-0337 (2015).

[17] P. Baudrenghien et al, *SPS LLRF upgrade specification cost manpower and schedule*, EDMS 1547550.

[18] LIU-SPS Fast Rise Time Injection System for Pb Ions Review, CERN, October 4th, 2013 https://indico.cern.ch/event/263338/overview.

7 Options

7.1 Introduction

Some additional improvements are under study to possibly push further the ion performance and even allow some margin for, as examples, reduced availability, or a lower number of colliding pairs (e.g. for filling schemes that meet all requirements, including, possibly, collisions at the LHCb experiment). The listed items are "LIU options", which would imply an extension of the baseline scenario with the additional hardware installation/modifications, and cost related.

- Implement the 100 ns rise time upgrade of the SPS injection kicker. This option was the first one to be investigated (hence the advanced stage of the study), and has since lost much of its attractiveness because of the successful implementation of the 150 ns spacing between batches in the SPS in 2015 (see Section 6.2). For 12 injections into SPS, 100 ns injection kicker gap would allow 1248 bunches in LHC, which is only about 8% more than the 1152 bunches possible with 100 ns. Additionally, it is also technically difficult, as discussed in detail in the following section;
- Use alternative PS production schemes, mainly leading to 25 ns spacing in LHC (e.g. batch compression or further splitting to 50 ns at the PS flat top). The potential use of these schemes depends on whether the available crossing angle at ALICE is adequate for 25 ns bunch spacing instead of 50 ns, a question requiring further study, as well as technical feasibility in the PS. In particular, only one scenario, which has been found to hold promise, will be singled out and analysed further in terms of achievable performance in one of the next sections;
- Reduce somewhat the LHC injection/dump kickers' gaps to realistic optimized values, and optimize the filling schemes accordingly to maximize the numbers of colliding bunches;
- Reduce the LEIR cycling period to 2.4 s, or possibly 3.0 s. Here it is believed that the main performance improvement would stem from: 1) the shorter injection plateau in LEIR preserving the present seven injections, and 2) the shortened SPS and LHC injection plateaux, which would entail an important mitigation of the low energy losses in these machines due to space charge, RF noise, IBS. While at the present stage the gain from this option has not yet been quantified, this will be further investigated before LS2 to determine its potential as well as the steps necessary to implement it.

Different sharing schemes, which could also help to meet the ALICE request, are not considered because the baseline is that ALICE, ATLAS and CMS are treated equally in terms of delivered luminosity.

7.2 SPS injection improvements: 100 ns injection kicker rise time

7.2.1 Scope and Introduction

The ion scheme used in the SPS, up to LS1 in 2013, made use of 12 injections of 2 bunches. The 12 batches were spaced by 200 ns for the SPS Q26 optics or by 225 ns for the Q20 optics. There have been 15 injections from the SPS to the LHC, leading to a total of 358 bunches injected in the LHC as used for the 2011 Pb-Pb ion run [1]. Since this, the injection kicker rise time has been improved, and together with the deployment of the transverse damper at injection (Chapter 6), has allowed injection into the SPS with 150 ns batch spacing, leading to 518 bunches injected into LHC for operation in 2015. This demonstrated performance will be approximately doubled to 1152 bunches in LHC, with the advent of slip-stacking in the SPS (see Table 1.2).

Several alternative ion schemes have been studied in the past [2]. Among them, the highest luminosity could be reached by reducing the SPS injection kicker rise time to 50 ns. However, taking into account arguments on the technical feasibility, beam impedance and the investments involved, an LIU-SPS

Internal Review in October 2013 decided [3] to further develop the option with the following characteristics:

- SPS injection kickers with a 100 ns rise time, measured from 2 – 98 %, and a flat top of at least 305 ns [3];
- New MSI-V septum, based on existing Booster BT septa;
- New ion dump.

Further details on the corresponding ion scheme can be found in [4]. The conceptual technical implementation for an injection system for 100 ns kicker rise time is described in the following sections.

7.2.2 Proposed system layout and parameters

To inject with 100 ns rise time only the MKP-S type injection kicker magnets would be used, powered by new PFLs in parallel to the present PFN system. Additional septa, MSI-V, are needed to compensate for the reduced MKP kick strength. A new dedicated ion injection dump is also required.

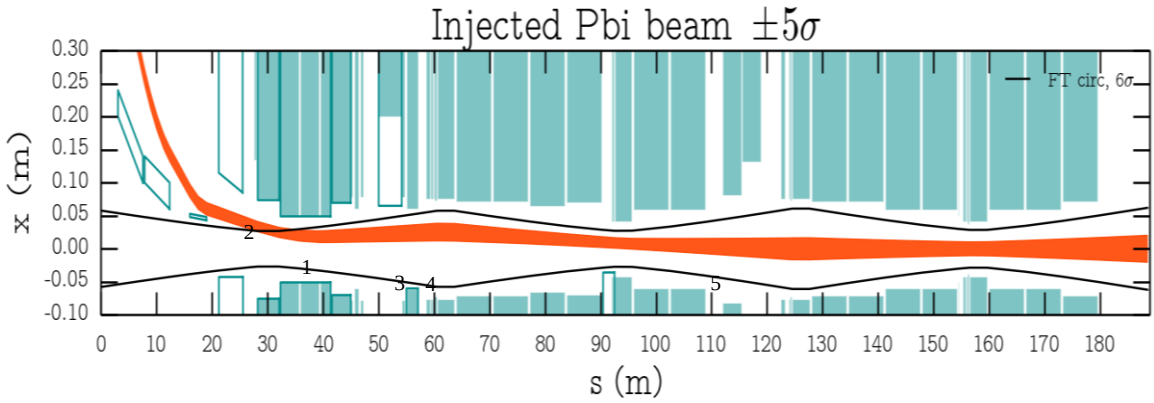

Figure 7.1 +/- 5 σ ion beam envelope following the foreseen injection trajectory.

The injection also needs a closed injection bump, which should have maximum amplitude at the QF.120 of 25 mm; this is obtained using 3 horizontal correctors. Figure 7.1 shows the nominal beam trajectory foreseen for the ion beam. The required new/modified elements and parameters are summarised in Table 7.1.

Table 7.1 Ion Injection Element Parameters.

#	Element	Magnetic Length	Deflection	B.dl
1	MSI-V (2 magnets)	1.5 m (per magnet)	12.3 mrad (full)	0.739 T.m
2	MSI (4 magnets)	2.1 m (per magnet)	42.8 mrad (full)	2.572 T.m
3	MKP-A (2tanks)	3.423 m (5 magnets)	0.862 mrad (tank)	0.052 T.m
4	MKP-C (1 tank)	1.78 m (2 magnets)	0.345 mrad (tank)	0.021 T.m
5	Ion Dump	-	-	-
1	BLM MSI-V	-	-	-

5	BLM Ion Dump	-	-	-
5	Ion Dump BTV/SEM	-	-	-

The aperture of the injection region for ion and proton beams has been checked in simulation [5]; the expected minimum aperture for the injected ion is 5.0 σ at the exit of the MSI-V. For the injected FT beam the MSI-V does not introduce any aperture limitation compared to the MSI exit and is around 4 σ. At the new MSI-V the aperture for FT-beam injection is about 7.5 σ. The MSI-V stability needs to be about 500 ppm to for emittance preservation reasons [6].

7.2.3 Injection System elements

Septum Magnets MSI-V: The proposed injection mechanism utilises an already existing design for the septum MSI-V, which is currently in use in the PS booster as part of the vertical recombination system. These will be housed in new tanks and powered with new converters.

Fast Pulsed Magnet System MKP: The MKP performance requirements need to be achieved by a pulse generator upgrade. A pulse forming line (PFL) will be used to power the MKPS magnets for ion injection only. There will be one PFL per 2 magnets, as is also the case for the present PFN, leading to a total of 6 PFLs.

Injection Dump: An injection dump specifically for ions, located between the MBB 12090 and the QD12110 is needed. The MBB 12070 and MBB 12090 would require a 10 mm horizontal offset which would allow the ion beam to be dumped. Initial feasibility studies have been performed for the ion beam parameters and a composite water-cooled block will be needed.

Beam Instrumentation: an additional beam screen and camera is needed to monitor the dumped beam. Additional BLMS will be required at the MSI-V and new ion dump, and the BPMs in the injection region need to be able to measure individual ion bunches.

Interlocking and machine protection: a reliable software interlock and fast current change monitor on the MSI should be foreseen in order to avoid a direct impact of the proton beam on the MSI-V. A reliable interlocking of the MSI-V, also based on hardware, is highly recommended. The effectiveness of an absorber protecting the upstream side of the MSI-V needs to be considered.

7.3 50 ns batch production in the PS

Except the two-bunch schemes with 100 ns and 200 ns spacing mentioned in Chapter 5, none of the alternative options that will be discussed in this subsection has yet been successfully tested or set-up with beam in the PS.

Beam tests in 2012 to split two bunches into four at the flat-top resulting in 50 ns bunch spacing, revealed important difficulties with adiabaticity due to the vicinity of transition. Two bunches were injected into $h = 16$ and then batch compressed to $h = 21$ as described in Chapter 5. At the flat-top it was tried to split the two bunches spaced by 100 ns from $h = 21$ to 42, the latter being generated by a slightly detuned 20 MHz cavity normally operated for protons. This manipulation failed due to the small bucket filling factor, as well as insufficient adiabaticity with the low synchrotron frequency. The same difficulty would apply to a bunch splitting of the nominal four-bunch beam to eight bunches spaced by 50 ns. Additionally, a further bunch splitting in the PS would require doubling the intensity from LEIR. Possibilities to lower the transition energy by optics changes are under study to increase synchrotron frequency and bucket filling factor. Alternatively, the extraction energy could be decreased well below transition in the PS to improve adiabaticity. However, already at the present transfer energy, the beam

suffers from intra-beam scattering, space charge and RF noise at the 40 s long flat-bottom in the SPS, which rules out lower injection energies.

Since bunch splitting seems challenging with ions on the flat-top unless the transition energy can be lowered significantly, batch compression or expansion techniques could be applied. These manipulations suffer less from adiabaticity issues as no part of the bunch distribution has a local low synchrotron frequency, nor is excessive precision in terms of relative phase during harmonic number hand-overs needed.

The 50 ns bunch spacing could hence also be achieved by batch compression. Starting from two bunches at a distance of 100 ns, they could be moved closer together by applying RF voltage at h = 7 and 21 simultaneously [7]. Once the bunches have been approached sufficiently close, they can be handed over in adjacent buckets at h = 42 generated by an RF cavity at 20 MHz which yield two bunches spaced by 50 ns. The existing 20 MHz cavity for protons detuned to a slightly lower frequency could be used to study this RF manipulation experimentally. For operational exploitation of this alternative, the installation of an additional 20 MHz cavity should be considered.

For the case of four bunches with a spacing of 50 ns, a significantly more complicated batch compression RF manipulation would be required on the flat-top. Starting from four bunches at 100 ns as for the nominal scheme, a batch compression with the harmonic number sequence $h = 21 \rightarrow 25 \rightarrow 30 \rightarrow 36 \rightarrow 42$ could be envisaged. The intermediate harmonic number steps are indicative. However, the installation of a completely new RF cavity covering the frequency range of 10 to 20 MHz, with the associated high-power and low-level hardware, would be needed. Thanks to the low longitudinal emittance, the vicinity of transition energy and the low intensity of the ion beam, the requirements and terms of voltage and feedback would be moderate.

The RF voltage at h = 42 will be insufficient though to adiabatically shorten the bunches for a direct re-bucketing into the 12.5 ns long buckets at h=169 for the final bunch compression with the 80 MHz RF system. This lack of RF voltage may be overcome by introducing an intermediate compression step at 40 MHz or by rotating the bunches from the h = 42 into the h = 169 buckets.

The scenario based on batch compression of four bunches at top energy in the PS has been found to be of two-fold interest, because it can: 1) provide up to 40% larger number of bunches (i.e. 1680 instead of 1152) in LHC with the same parameters as in the LIU baseline scenario, and 2) be an efficient mitigation against a possible underperformance of the slip stacking in the SPS or a longer set up time than anticipated.
To have an overview on the ion beam performance throughout the injector chain, the relevant beam parameters at the various stages of the LHC ion injector synchrotrons (i.e. at injection and extraction from each machine) for the different scenarios have been summarised in Table 7.2. In particular, here is a more detailed explanation of the different lines:

- ‘Achieved 2015’: average values measured in 2015;
- ‘LIU-ions’: values achievable with the LIU baseline upgrades;
- ‘LIU-ions 25 ns’: achievable values if 50ns PS batch compression is included in the upgrade program;
- ‘HL-LHC’: requested HL-LHC parameters.

Furthermore, also the estimated number of bunches in LHC, the LHC filling time and the total number of ions at the end of the injection process in LHC for each of these scenarios have been reported in the table (bottom right). Comparing the ‘HL-LHC’ scenario with the analysed upgrade scenarios, one can conclude that, while ‘LIU-ions’ offers 20% lower bunch intensities at the SPS extraction and 8% fewer bunches in LHC (with a potential loss of integrated luminosity in LHC around 20%, depending on the LHC performance efficiency), ‘LIU-ions 25 ns’ can compensate the 20% lower bunch intensities with up to 35% more bunches in LHC. In fact, although the LHC filling time becomes about 33% longer, the

total number of ions at the end of the injection process in the LHC, which gives a first order estimate of the achievable integrated luminosity, is actually highest for the alternative 'LIU-ions 25 ns' scenario, suggesting that it can meet the final requirement of integrated luminosity during the post-LS2 era with some margin.

Table 7.2 Summary of the ion beam parameters in different scenarios.

	N_{ions}/bunch (10^8)	$\varepsilon_{x,y}$ (μm)	Bunches /injection	Bunch spacing (ns)	N_{ions}/bunch (10^8)	$\varepsilon_{x,y}$ (μm)	Bunches	Bunch spacing (ns)
LEIR	**Before RF capture (54^+, E_{kin}=0.0042 GeV/u)**				**Extraction (54^+, E_{kin}=0.0722 GeV/u)**			
Achieved	15.5	0.1, 0.4	coasting beam		6.0		2	354
LIU-ions	18.6				7.4		2	354
LIU-ions 25 ns	18.6				7.4		2	354
HL-LHC	29.5				11.8		2	354
PS	**Injection (54^+, E_{kin}=0.0722 GeV/u)**				**Extraction (54^+, E_{kin}=5.9 GeV/u)**			
Achieved	5.5		2	354	5.1	0.9, 0.8	2	100
LIU-ions	6.8		2	354	3.1	1.0	4	3x100
LIU-ions 25 ns	6.8		2	354	3.1	1.0	4	3x50
HL-LHC	10.9		2	354	5.0	1.0	4	3x100
SPS	**Injection (82^+, E_{kin}=5.9 GeV/u)**				**Extraction (82^+, E_{kin}=176.4 GeV/u)**			
Achieved	4.3	1.0, 0.9	2	100	2.2		24	11x(100+150)+100
LIU-ions	2.6	1.0	4	3x100	1.7	1.3	48	5x(7x50+100)+7x50
LIU-ions 25 ns	2.6	1.0	4	3x50	1.7	1.3	56	6x(7x25+125)+7x25
HL-LHC	4.2	1.0	4	3x100	2.1	1.3	48	47x50

LHC	**Injection (82^+, E_{kin}=176.4 GeV/u)**			LHC filling time	Total number of bunches	Total number of ions after injection
Achieved	2.2	1.5	24	40 (60) min	518	–
LIU-ions	1.7	1.3	48	43 min	1152	2.0×10^{11}
LIU-ions 25 ns	1.7	1.3	56	60 min	1680	2.8×10^{11}
HL-LHC	2.1	1.3	48	45 min	1248	2.6×10^{11}

7.4 References

[1] J.M. Jowett et al, *Heavy ions in 2012 and the programme up to 2022*, in Proc. of Chamonix 2012 workshop on LHC performance, p.200, CERN-ATS-2012-069 (2012).

[2] D. Manglunki et al, *Motivation for 50 ns rise time injection*, LIU-SPS 50 ns Injection System for Pb ions Review, CERN, October 2013.

[3] M. Benedikt et al, *LIU-SPS 50 ns Injection Review, Executive Summary*, CERN October 2013, EDMS 1331860.

[4] D. Manglunki, *Provisional list of parameters for ions in HL-LHC*, Technical Specification, 07-07-2014, CERN EDMS 1311644.

[5] F. M. Velotti et al, *Aperture and failure scenarios*, LIU-SPS 50 ns Injection System for Pb ions Review, CERN October 2013.

[6] F.M. Velotti, T. Kramer and J. Uythoven, *Transverse emittance blow-up of the heavy ion beam injected into the SPS from the proposed MSI-V septum*, CERN-ACC-NOTE-2015-0030 (2015).

[7] C. Carli, private communication, 2013.